6

Mass Transfer Between Clusters Under Ostwald's Ripening

Roman Vengrenovich, Bohdan Ivanskii,
Anatolii Moskalyuk, Sergey Yarema and Miroslav Stasyk
Chernivtsi National University after Yu. Fed'kovich, Chernivtsi, Ukraine

1. Introduction

Decay of oversaturated solid solutions with forming a new phase includes three stages, *viz.* nucleation of centers (clusters, nucleation centers, extractions), independent growth of them and, at last, development of these centers interconnecting to each other. This last stage, so-called late stage of decay of oversaturated solid solution has been firstly revealed by Ostwald (Ostwald, 1900). Its peculiarity consists in the following. Diffusion mass transfer of a matter from clusters with larger magnitudes of surface curvature to ones with smaller magnitudes of surface curvature (owing to the Gibbs-Thomson effect) results in dissolving and disappearing small clusters that causes permanent growth of the mean size of extractions. In accordance with papers (Sagalovich, Slyozov, 1987; Kukushkin, Osipov, 1998), interaction between clusters is realized through the 'generalized self-consistent diffusion field'. This process, when large clusters grow for account of small ones is referred to as the Ostwald's ripening. Investigation of the Ostwald's ripening resulted in determination of the form of the size distribution function in respect of the mass transfer mechanisms. The first detailed theory of the Ostwald's ripening for the diffusion mass transfer mechanism has been developed by Lifshitz and Slyozov (Lifshitz and Slyozov, 1958, 1961). Under diffusion mass transfer mechanism, atoms of a solved matter reaching clusters by diffusion are then entirely absorbed by them, so that cluster growth is controlled by matrix diffusion and, in part, by the volume diffusion coefficient, D_v. In paper (Wagner, 1961), Wagner has firstly showed that it is possible, if the atoms crossing the interface 'cluster-matrix' and falling at a cluster surface in unit of time have a time to form chemical connections necessary for reproduction of cluster matter structure. If it is not so, solved atoms are accumulated near the interface 'cluster-matrix' with concentration C that is equal to the mean concentration of a solution, $\langle C \rangle$. For that, growing process is not controlled by the volume diffusion coefficient, D_v, but rather by kinetic coefficient, β. Thus, in his paper published three years later than the papers by Lifshitz and Slyozov, Wagner considered other mechanism of cluster growth controlled by the rate of formation of chemical connection at cluster surface. The quoted papers (Lifshitz, Slyozov, 1958, 1961; Wagner, 1961) form the base of the theory of the Ostwald's ripening that is conventionally referred to as the Lifshitz-Slyozov-Wagner (LSW) theory. Within the framework of this theory, several

other problems connected with the Ostwald's ripening for diffusion at grain boundaries (Slyozov, 1967; Kirchner, 1971), for surface diffusion (Chakraverty, 1967; Vengrenovich, 1977), for diffusion along dislocation pipes (Ardell, 1972; Kreye, 1970; Vengrenovich, 1975, 1982; Vengrenovich *et al.*, 2001a, 2002) etc. have been solved later. A new phase extracted during decay of oversaturated solid solution as specific matrices of particles (clusters) is the strengthening phase. Its extractions act as a stopper for traveling dislocations. Elastic strength fields arising around clusters and interacting with matrix dislocations, depending on their energy, can be fixed at cluster surfaces or cut of them. Cutting the extracted particles (clusters) by dislocations or fixing of them at particle surfaces leads to the pipe mechanism of diffusion along dislocations with diffusion coefficient D_d (Vengrenovich, 1980a, 1980b, 1983; Vengrenovich *et al.*, 1998).

For some time past, the LSW theory is successfully used for analysis of evolution of island structure resulting from self-organization in semiconductor heterosystems (Bartelt *et al.*, 1992, 1996; Goldfarb *et al.*, 1997a, 1997b; Joyce *et al.*, 1998; Kamins *et al.*, 1999; Vengrenovich *et al.*, 2001b, 2005, 2010; Pchelyakov *et al.*, 2000; Ledentsov *et al.*, 1998; Xiaosheng Fang *et al.*, 2011). It is also used for dscription of dissipative structures in non-equilibrium semiconductor systems (Gudyma, Vengrenovich, 2001c; Vengrenovich *et al.*, 2001d).

Mass transfer between clusters under the Ostwald's ripening depends on the kind of diffusion than, in its turn, determines the rate of growth of clusters and the size distribution function of them. As it has been noted above, the size distribution function of clusters for matrix diffusion mechanism has been for the first time obtained by Lifshitz and Slyozov within the framework of hydrodynamic approximation. So, this distribution is referred to as the Lifshitz-Slyozov distribution.

This chapter is devoted to the computing of the size distribution function of clusters under mass transfer corresponding to simultaneous (combined) action of various diffusion mechanisms. Topicality of this study follows from the fact that often in practice (due to various reasons) mass transfer between clusters is controlled in parallel, to say, by the kinetic diffusion coefficient, β, and by the matrix diffusion coefficient D_v, or, alternatively, by the coefficients D_v and D_d, simultaneously, ect. All following computations are carried out within the Lifshitz-Slyozov hydrodynamic approximation using the approach developed earlier by one of the authors of this chapter (Vengrenovich, 1982).

2. Cluster growth under diffusion and Wagner mechanisms of mass transfer. Generalized Lifshitz-Slyozov-Wagner distribution

Following to Wagner, the number of atoms crossing the interface 'cluster-matrix' and getting to the cluster surface in unite of time, j_1, is

$$j_1 = 4\pi r^2 \beta \langle C \rangle , \tag{1}$$

and the number of atoms leaving it in unite of time is

$$j_2 = 4\pi r^2 \beta C_r , \tag{2}$$

so that the resulting flux of atoms involving into formation of chemical connections is

$$j_i = j_1 - j_2 = 4\pi r^2 \beta \left(\langle C \rangle - C_r \right) , \tag{3}$$

where $C_r = C_\infty \exp\left(\frac{2\sigma\upsilon_m}{kTr}\right) \approx C_\infty\left(1+\frac{2\sigma\upsilon_m}{rkT}\right)$ – concentration of atoms of solved matter at the boundary of a cluster of radius r, C_∞ – equilibrium concentration for specified temperature T, σ – interface surface energy, υ_m – volume of an atom of solved matter, and k – the Boltzmann constant.

The flows j_1 (Eq. 1) (to the cluster) and j_2 (Eq. 2) (from the cluster) are caused by thermal motion of atoms. j_1 in Eq. 1 is proportional to the mean concentration of the solution, $\langle C\rangle$. j_2 in Eq. 2 is proportional to concentration C_r, that is set at the cluster boundary in accordance with the Gibbs-Thomson formula: ($C_r = C_\infty \exp\left(\frac{2\sigma\upsilon_m}{kTr}\right)$).

Both in j_1 (Eq. 1) and in j_2 (Eq. 2), the kinetic diffusion coefficient equals the flow density for the unit concentration. Thus, taking into account the nature of flows, the kinetic diffusion coefficients are regarded to be equal to each other in j_1 and in j_2.

Introducing the kinetic coefficient, β, determining the flow j_i is caused by non-equilibrium character of the processes occurring both at the cluster surfaces and at their interfaces with a matrix. On this reason, one can not write the flow j_i through the concentration gradient at the interface. Formally, it can be represented through concentration gradient:

$$j_i = 4\pi r^2\beta\left(\langle C\rangle - C_r\right) = 4\pi r^2\beta r\frac{\langle C\rangle - C_r}{r}, \tag{4}$$

where $\beta\cdot r$ has a dimension of the diffusion coefficient; however, such diffusion coefficient, $D^* = \beta r$, has no physical sense. That is why, one proceeds to the kinetics.

In equilibrium state one has:

$$j_i = j_v = j, \tag{5}$$

that is why the flow j of atoms to (from) a cluster can be determined as

$$j = \frac{1}{2}\left(j_i + j_v\right), \tag{6}$$

where j_v – the number of atoms reaching a cluster surface in unite of time through diffusion.

In general case, the flow j of atoms to (from) a cluster will be

$$j = j_i + j_v. \tag{7}$$

The flow j in Eq. (7) provides determination of the rate of cluster growth.

2.1 The rate of cluster growth

For determining the size distribution function of particles, $f(r,t)$, one must know the rate of particle's growth, $\dot{r} = \frac{dr}{dt}$, that is connected with the size distribution function of the continuity equation:

$$\frac{\partial f(r,t)}{\partial t}+\frac{\partial}{\partial r}\left(f(r,t)\dot{r}\right)=0\,. \tag{8}$$

The rate of cluster growth is determined from a condition:

$$\frac{d}{dt}\left(\frac{4}{3}\pi r^3\right)=j\upsilon_m\,, \tag{9}$$

where j is determined by Eq. (7). There is the diffusion part of a flow:

$$j_v=4\pi r^2 D_v\left(\frac{dC}{dr}\right)_{R=r}=4\pi r^2 D_v\frac{\langle C\rangle-C_r}{r}\,. \tag{10}$$

Taking into account Eqs. (3) and (10), one finds from Eq. (9):

$$\frac{dr}{dt}=\frac{\left(\langle C\rangle-C_r\right)\upsilon_m}{4\pi r^2}\left(4\pi r^2\beta+4\pi r^2 D_v\frac{1}{r}\right). \tag{11}$$

Let us denote the shares j_v and j_i in general flow j as x and $(1-x)$, respectively:

$$x=\frac{j_v}{j}\,,\ 1-x=\frac{j_i}{j}\,,\ \frac{j_v}{j_i}=\frac{x}{1-x} \tag{12}$$

To represent the rate of growth (11) through the share flows j_i and j_v, let us take out of the brackets the second term, $4\pi r^2 D_v\frac{1}{r}$, and multiply nominator and denominator of the firs term by $\left(\langle C\rangle-C_{r_g}\right)r_g^2$, where C_{r_g} is the concentration at the boundary with a cluster of maximal size r_g:

$$\frac{dr}{dt}=\left(\langle C\rangle-C_r\right)\frac{D_v\upsilon_m}{r}\left(\frac{4\pi r_g^2\beta\left(\langle C\rangle-C_{r_g}\right)}{4\pi r_g^2 D_v\dfrac{\left(\langle C\rangle-C_{r_g}\right)}{r_g}}\frac{r}{r_g}+1\right). \tag{13}$$

The ratio $\dfrac{4\pi r_g^2\beta\left(\langle C\rangle-C_{r_g}\right)}{4\pi r_g^2 D_v\dfrac{\left(\langle C\rangle-C_{r_g}\right)}{r_g}}$ equals the ratio of the flows $\frac{j_i}{j_v}$ for a particle of the maximal size, and, in accordance with Eq. (12), it can be replaced by $\left(\frac{1-x}{x}\right)$, while there are not any limitations on particle size in Eq. (12). Besides, taking into account that $\langle C\rangle-C_r=\frac{2C_\infty\sigma\upsilon_m}{kT}\left(\frac{1}{r_k}-\frac{1}{r}\right)$, the rate of growth (13) can be rewritten in the following form:

$$\frac{dr}{dt}=\frac{\sigma C_\infty \upsilon_m^2 D_v}{kT}\frac{1}{r^2}\left(\frac{1-x}{x}\frac{r}{r_g}+1\right)\left(\frac{r}{r_k}-1\right), \tag{14}$$

where r_k is the critical radius. Within the LSW theory, r_k coincides with a mean size of particles, $r_k=\langle r\rangle$.

Eq. (14) corresponds to the rate of cluster growth through matrix diffusion with the share contribution $(1-x)$ of the part of flow controlled by the kinetic coefficient β. For $x=1$, Eq. (14) coincides with the rate of growth Eq. (2.15) from the review paper (Sagalovich, Slyozov, 1987), *viz.* $\left(\frac{dR}{dt}=\frac{D_{n-1}a_{n-1}}{R^{n-1}}\left(\frac{R}{R_k}-1\right)\right.$, where $\left.\Delta=\frac{\alpha}{R_k}\right)$ for $n=3$, where $D_2=D_v$, $a_2=\frac{C_\infty\sigma\upsilon_m^2}{kT}$.

Repeating this procedure and taking out of the brackets $4\pi r^2\beta$, one obtains:

$$\frac{dr}{dt}=\frac{C_\infty\sigma\upsilon_m^2\beta}{kT}\frac{1}{r}\left(\frac{x}{1-x}\frac{r_g}{r}+1\right)\left(\frac{r}{r_k}-1\right). \tag{15}$$

Eq. (15) determines the rate of cluster growth under conditions controlled by the kinetic coefficient β with the share contribution x of matrix diffusion. If $x=0$, then growth is fully determined by the kinetic coefficient, and our Eq. (15) coincides with Eq. (2.15) form (Sagalovich, Slyozov, 1987) for $n=2$, where, $D_1=\beta$, $a_1=\frac{C_\infty\sigma\upsilon_m^2}{kT}$. In Eqs. (14) or (15) for the rate of growth that are the combinations of the Wagner and conventional diffusion mechanisms of cluster's enlargement, one assumes that no any term in the general flow j, Eq. (7), can be neglected. It means that the flows j_v and j_i must be commensurable. However, the intrigue consists in that formation of chemical connections is electron process, while the classical diffusion is the atomic activation process with considerably different temporal scale. Thus, the question arises: what are the conditions for two qualitatively different relaxation times, $\tau_{chem.con.}$ and $\tau_{diffus.}$, become comparable to each other? Thus the question on the ratio of flows j_v and j_i is reduced, in fact, to the ratio of the relaxation times $\tau_{chem.con.}$ and $\tau_{diffus.}$, and, as a result, to the question on the possibility to implement the proposed mechanism of cluster growth. To obtain answer on this question is, in general, too hardly.

To all appearance, the relaxation times $\tau_{chem.con.}$ and $\tau_{diffus.}$ are commensurable, if the electron process of formation of chemical connections is activation one, and if the activation energies for both processes (electron and diffusion) are comparable.

In paper (Wagner, 1961), the solution is obtained for the limiting cases: $x=0$, $\tau_{diffus.} << \tau_{chem.con.}$, (the Wagner mechanism of growth), and, $x=1$, $\tau_{chem.con.} << \tau_{difus.}$, (the diffusion mechanism of growth). Note, Wagner (Wagner, 1961) does not discuss the relaxation times.

In the case under consideration here, when the solution is found for arbitrary magnitude of x within the interval $0<x<1$, relaxation times must be comparable to each other at least for the systems whose histograms are represented by the computed curves. We provide this comparison below.

2.2 Temporal dependences of r_g and r_k

One of the main parameters of the LSW theory is the ratio r_g/r_k (in terms of the papers (Lifshitz and Slyozov, 1958, 1961), locking point u_0), whose magnitude together with the equation for the rate of growth (14) or (15) provides integration of Eq. (8) after separation of variables and determination of the analytical form of the size distribution function. This ratio can be determined from the dependence of the specific rate of growth $\dot{r}/r$ on r, that is schematically shown in Fig. 1, where $\dot{r}$ is determined by Eq. (14) or (15) (Vengrenovich, 1982).

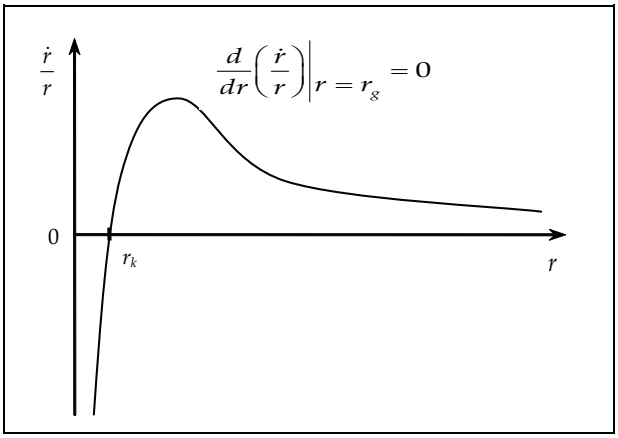


Fig. 1. Schematic dependence of the specific rate of growth $\frac{\dot{r}}{r}$ on r

At the point where the rate of growth on the unite length of cluster radius reaches its maximal magnitude, derivation equals zero:

$$\left.\frac{d}{dr}\left(\frac{\dot{r}}{r}\right)\right|_{r=r_g} = 0\,. \tag{16}$$

From the physical point of view, it means that the maximal size of r_g is reached for the particle, for which the rate of growth of the unit of length of its radius is maximal. Thus, one obtains from Eq. (16):

$$\frac{r_g}{r_k} = \frac{2+x}{1+x}\,. \tag{17}$$

Assuming in Eq. (14) $r = r_g$ and replacing the ratio $\frac{r_g}{r_k}$ by its magnitude from Eq. (17), one obtains by integration:

$$r_g^3 = A^* \frac{t}{x(1+x)}\,, \tag{18}$$

where, $A^* = \frac{3\sigma \upsilon_m^2 C_\infty D_v}{kT}$, or:

$$r_k^3 = A^* \frac{(1+x)^2}{x(2+x)^3} t \,. \tag{19}$$

For $x = 1$ particle growth is full controlled by the volume diffusion coefficient:

$$r_g^3 = \frac{1}{2} A^* t \,,\; r_k^3 = \frac{4}{27} A^* t \,,\; \frac{r_g}{r_k} = \frac{3}{2} \,. \tag{20}$$

By analogy, one obtains from Eq. (15):

$$r_g^2 = B^* \frac{t}{1-x^2} \,, \tag{21}$$

where $B^* = \frac{2\sigma \upsilon_m^2 C_\infty \beta}{kT}$, or:

$$r_k^2 = B^* \frac{1+x}{(1-x)(2+x)^2} t \,. \tag{22}$$

Eqs. (21) and (22) describe changing in time cluster sizes, when growth of them is controlled by the kinetic coefficient β, with the share contribution x of matrix diffusion. If $x = 0$, then the process of growth is fully controlled by kinetics of transition through the interface 'cluster-matrix':

$$r_g^2 = B^* t \,,\; r_k^2 = \frac{1}{4} B^* t \,,\; \frac{r_g}{r_k} = 2 \,. \tag{23}$$

2.3 Size distribution function

The size distribution function, $f(r,t)$, and the rate of growth, $\dot{r}$, are connected by the continuity equation (8). Knowing $\dot{r}$ (Eqs. (14) or (15)), one can find $f(r,t)$ from Eq. (8). Following to paper (Vengrenovich, 1982), $f(r,t)$ is found as the product:

$$f(r,t) = \varphi(r_g) g'(u) \,, \tag{24}$$

where $g'(u)$ is the relative size distribution function of clusters, $u = \frac{r}{r_g}$.

To determine the function $\varphi(r_g)$, let us apply the conservation law for mass of disperse phase:

$$M = \frac{4}{3} \pi \rho \int_0^{r_g} r^3 f(r,t)\, dr \,, \tag{25}$$

by substituting in it $f(r,t)$ from Eq. (24):

$$\varphi\left(r_g\right)=\frac{Q}{r_g^4}, \tag{26}$$

where $Q=\dfrac{M}{\dfrac{4}{3}\pi\rho\int_0^1 u^3 g'(u)\,du}$.

Substituting Eq. (26) in Eq. (24), one obtains:

$$f(r,t)=\frac{Q}{r_g^3}g'(u)=\frac{g(u)}{r_g^3}, \tag{27}$$

where:

$$g(u)=Q\cdot g'(u). \tag{28}$$

The relative size distribution function $g'(u)$ is determined from the continuity equation. For that, one substitutes in Eq. (8) the magnitude $f(r,t)$ from Eq. (24) and takes into account Eq. (26), as well as the magnitude of $\dot{r}$ from Eqs. (14) or (15). After the mentioned substitution and transition in Eq. (8) from differentiation on r and t to differentiation on $u=\dfrac{r}{r_g}$ ($\dfrac{\partial}{\partial r}=\dfrac{\partial}{\partial u}\dfrac{du}{dr}$, where $\dfrac{du}{dr}=\dfrac{1}{r_g}$; $\dfrac{\partial}{\partial t}=\dfrac{\partial}{\partial u}\dfrac{du}{dr_g}\dfrac{dr_g}{dt}$, where $\dfrac{\partial u}{\partial r_g}=-\dfrac{u}{r_g}$), the variables are separated, and Eq. (8) takes the form:

$$\frac{dg'(u)}{g'(u)}=-\frac{4\upsilon_g-\dfrac{1}{u^2}\dfrac{d\upsilon}{du}+2\dfrac{\upsilon}{u^3}}{u\upsilon_g-\dfrac{\upsilon}{u^2}}du, \tag{29}$$

where it is taken into account that:

$$\upsilon=\frac{r^2\dot{r}}{B^*}=\left(1+\frac{1-x}{x}u\right)\left(\frac{2+x}{1+x}u-1\right),\ \upsilon_g=\frac{r_g^2}{B^*}\frac{dr_g}{dt}=\upsilon\Big|_{u=1}=\frac{1}{x(1+x)}. \tag{30}$$

Substituting the magnitudes υ, υ_g and $\dfrac{d\upsilon}{du}$ into Eq. (29), after straightforward transformations one obtains:

$$\frac{dg'(u)}{g'(u)}=-\frac{4u^3+u\left(2x^2+2x-1\right)-2(1+x)x}{u(1-u)^2\left(u+x+x^2\right)}du. \tag{31}$$

Integration of Eq. (31) provides obtaining the analytical form of the generalized LSW distribution, which has been for the first time obtained by us (Vengrenovich *et al*., 2007b) :

$$g'(u)=u^2(1-u)^{-B}(u+x^2+x)^D\exp\left[\frac{C}{1-u}\right], \tag{32}$$

where

$$\begin{cases} B = \dfrac{2x^4 + 4x^3 + 12x^2 + 10x + 5}{A}, \quad C = -\dfrac{3x^2 + 3x + 3}{A}, \\ D = -\dfrac{4x^4 + 8x^3 + 6x^2 + 2x + 1}{A}, \; A = x^4 + 2x^3 + 3x^2 + 2x + 1. \end{cases} \tag{33}$$

For $x = 1$, $B = 11/3$, $C = -1$, $D = -7/3$ Eq. (32) corresponds to the Lifshitz-Slyozov distribution:

$$g'(u) = u^2 (1-u)^{-11/3} (u+2)^{-7/3} \exp\left(-\frac{1}{1-u}\right). \tag{34}$$

For $x = 0$, $B = 5$, $C = -3$, $D = -1$ Eq. (32) corresponds to the Wagner distribution:

$$g'(u) = u(1-u)^{-5} \exp\left(-\frac{3}{1-u}\right). \tag{35}$$

Within the interval $0 \le x \le 1$, the size distribution function is represented by the generalized LSW function. However, for graphic representation of the size distribution function one must compute following Eq. (28), where the conservation law for mass (volume) of a film is taken into account.

To obtain the distributions represented by Eqs. (34) and (35) in the form derived by Lifshitz and Slyozov (Lifshitz and Slyozov, 1958, 1961) and by Wagner (Wagner, 1961), one must go from the variable $u = \dfrac{r}{r_g}$ to the variable $\rho = \dfrac{r}{r_k}$: $u = \dfrac{r}{r_g} = \dfrac{r}{r_k}\dfrac{r_k}{r_g} = \dfrac{\rho}{u_0}$, where u_0 – the locking point ($u_0 = \dfrac{r_g}{r_k}$), and r_k – the critical radius.

2.4 Discussion

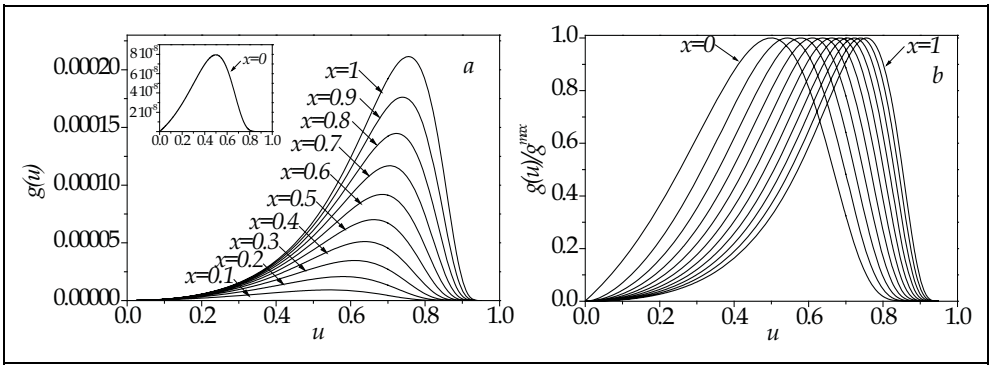


Fig. 2. The curves computed following Eq. (28): a – depending on *x*; b – normalized by maximal magnitudes

Fig. 2,a illustrates the curves corresponding to the distribution Eq. (28) computed for various magnitudes of the parameter x with interval $\Delta x = 0.1$. Inset shows the Wagner function $(x = 0)$, which is hardly to be shown in the main graph in its scale. One can see gradual

transition from the Lifshitz-Slyozov distribution, Eq. (34) $(x = 1)$, to the Wagner distribution, Eq. (35). The same curves normalized by their maxima are shown in Fig. 2, b. In this form, these curves are suitable for comparison with the corresponding normalized experimentally obtained histograms.

Note, that computation of the theoretical curve under simultaneous (combined) action of two mass transfer mechanisms, *viz.* volume diffusion and chemical reaction at the interface 'extraction-matrix' has been performed earlier by using numerical techniques (Sagalovich, Slyozov, 1987).

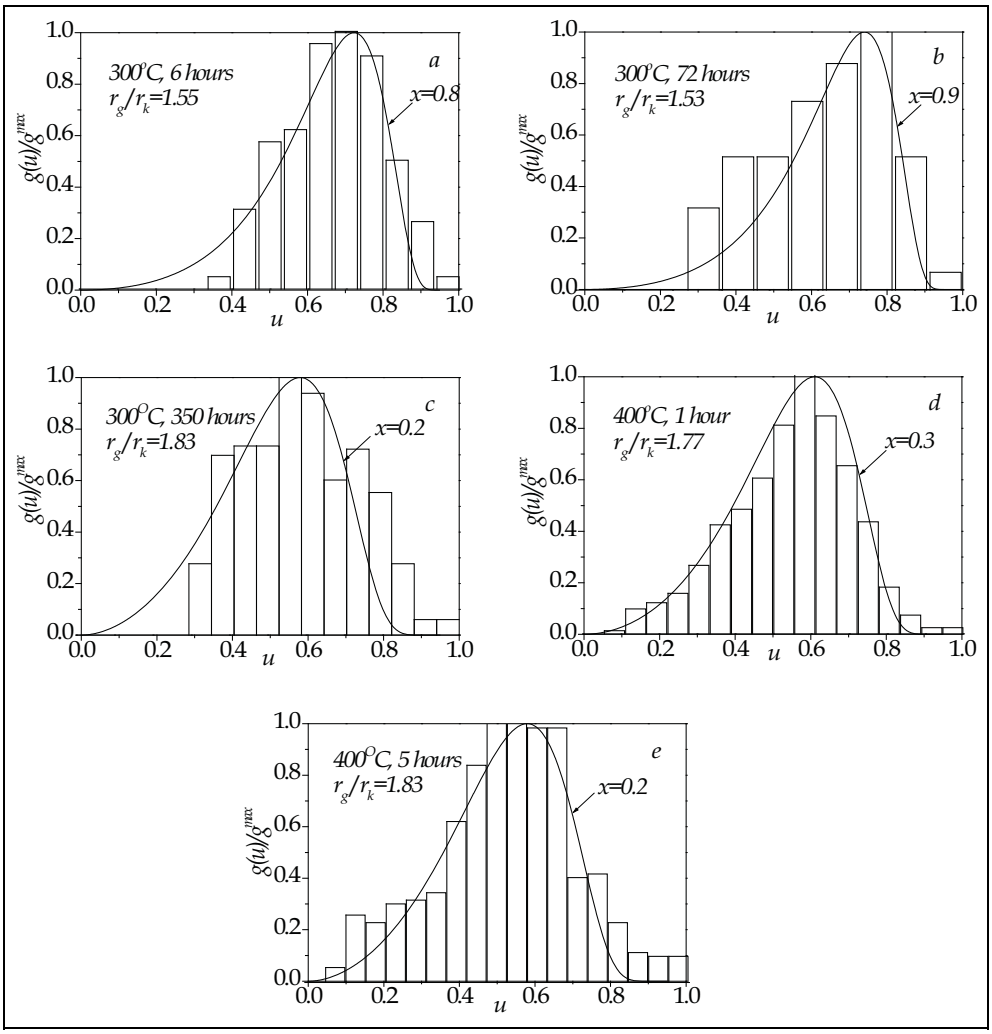


Fig. 3. Comparison of the dependence (28) with the experimentally obtained histograms of nano-scale particles Al_3Sc in alloys $Al-Sc$ (Marquis and Seidman, 2001) for various temperatures and exposure times shown in fragments a, b, c, d, and e

However, the distribution Eq. (28) computed for two mechanisms of mass transfer controlled by the volume diffusion coefficient and kinetics of transition of solved atoms through the interface 'cluster-martix', i.e. by the kinetic coefficient β, has been firstly obtained in analytic form by us. As the rate of forming the chemical connection is higher, as more simply solved atoms overcome potential barrier at the interface 'cluster-martix'. In this case, the rate of cluster growth is in less degree controlled by kinetics at the interface and in more degree by the diffusion processes of mass transfer. For that, the contribution of diffusion flow j_v in general flow of matter j to (from) a particle increases, and the size distribution function becomes more and more close to the Lifshitz-Slyozov distribution, Eq. (34).

Fig. 3 illustrates the results of comparison of the theoretical dependence, Eq. (28), with the experimentally obtained histograms of nano-scale particles Al_3Sc in alloys $Al-Sc$ (Marquis and Seidman, 2001) corresponding to temperature 300°C and exposure times *a* – 6, *в* – 72, *c* – 350 hours; to temperature 400°C and exposure times *d* – 1, *e* – 5 hours. Using the magnitudes of x from the results of comparison, one can determine percentage ratio between the flows $(x \cdot 100\%)$ and find, in this way, what mechanism is predominant.

Besides, knowing x, one can find the ratio $\frac{r_g}{r_k}$ that then may be used as the evaluation parameter for the choice of theoretical curve and comparison with desired histogram.

It follows from Fig. 3 that increasing of the exposure time for temperature 300°C up to 350 hours results in changing the mechanism of particle growth from one limited predominantly by diffusion processes of mass transfer, cf. fragments a – $x = 0.8$; b – $x = 0.9$, to one controlled predominantly by kinetics at the interface 'cluster-matrix', cf. fragment c – $x = 0.2$. Increasing the exposure temperature to 400°C leads to particle growth under conditions controlled predominantly by kinetics at the interface, cf. fragments d – $x = 0.3$; e – $x = 0.2$.

The possibility for implementation of the considered mechanism of particle growth controlled simultaneously both by the volume diffusion coefficient, D_v, and by the kinetic coefficient, β, is also proved by the experimentally obtained histograms for nano-crystals of aluminium obtained under crystallization of amorphous alloy $Al_{85}Ni_8Y_5Co_2$ (Nitsche *et al.*, 2005).

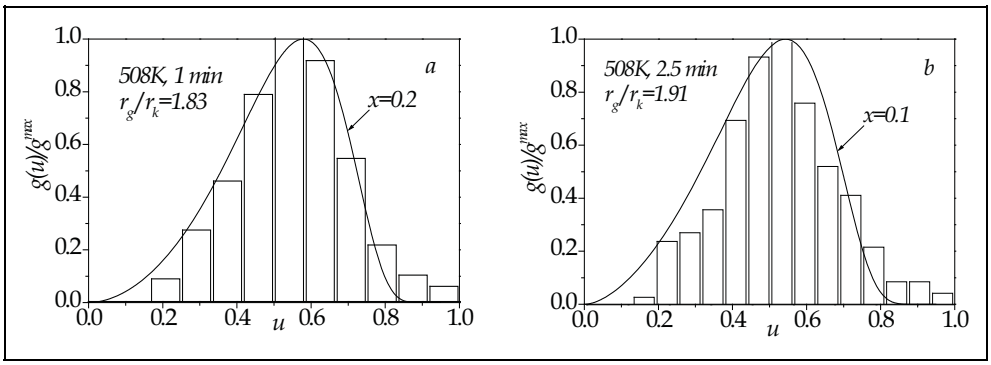


Fig. 4. Comparison with experimental histograms for nano-crystals Al, obtained under annealing of amorphous alloy $Al_{85}Ni_8Y_5Co_2$ (508°K) during: a – 1 min; b – 2.5 min (Nitsche *et al.*, 2005)

Fig. 4 shows comparison of the experimental histograms obtained under crystallization of amorphous alloy for temperature 508°K during 1 min and 2.5 min (fragments a and b, respectively) with the theoretical dependence, Eq. (28). One can see that theoretical dependences well fit the experimental histograms for $x = 0.2$ (fragment a) and $x = 0.1$ (fragment b).

Thus, the considered examples of comparison with the experimental data prove the conclusion that the distribution Eq. (28) is quite eligible for description of experimentally obtained histograms, if particle growth in the process of the Ostwald ripening is controlled simultaneously by two mechanisms of mass transfer, which earlier were considered separately by Lifshitz and Slyozov, and Wagner.

3. Cluster growth under dislocation-matrix diffusion. Size distribution function

The Ostwald's ripening of disperse phases in metallic alloys at the final stage of forming their structure reflecting the late stage of the development of nucleation centers of a new phase in time, when oversaturation between them decreases and their diffusion fields overlap.

In respect to metallic alloys strengthened by disperse extractions of the second phase, the Ostwald ripening is one of the causes of loss of strength of them. As large particles grow and small particles disappear (due to dissolution), distance between particles increases resulting in decreasing of tension necessary for pushing the dislocations between particles and, correspondingly, to decreasing of the creep strength.

For the dislocation mechanism of growth of particles that are coherent with a matrix, the flow along dislocations, j_d, much exceeds the flow of matrix diffusion, j_v:

$$D_d Z q \left(\frac{dC}{dR}\right)_{R=r} >> D_v 4\pi r^2 \left(\frac{dC}{dR}\right)_{R=r}, \tag{36}$$

where D_d, D_v – the coefficients of dislocation and matrix diffusion, respectively, Z – the number of dislocation lines that are fixed or crossing a particle of radius r, q – the square of dislocation pipe cross-section, $\left(\frac{dC}{dR}\right)_{R=r}$ – gradient of concentration at the boundary of a particle. Taking into account that for disturbed coherence (as a consequence of relaxation of elastic tensions (Kondratyev & Utyugow, 1987)) Z is not constant $(Z \neq const)$ being changed in inverse proportion to the particle radius, inequality (36) determines limitations on particle sizes for which the pipe mechanism of diffusion is yet possible (Vengrenovich *et al*., 2002):

$$r << \sqrt[3]{\frac{D_d Z_0 q^{3/2}}{4\pi^2 D_v}}, \tag{37}$$

where Z_0 is the initial number of dislocations fixed at particle surface. If the condition (37) is violated, it means that one can not neglect the component j_v caused by matrix diffusion in full flow of matter j to (from) a particle. In this case, particle growth takes place under diffusion of mixed type (dislocation-matrix one), when one can not neglect any of two components, j_d or j_v, in the resulting flow

$$j = j_d + j_v . \tag{38}$$

Below we represent the results of investigation of peculiarities of the Ostwald ripening of clusters under dislocation-matrix diffusion and, in part, computation of the size distribution function and temporal dependences for mean (critical) and maximal particle sizes as a function of the ratio of flows j_d and j_v .

3.1 The rate of growth and temporal dependences for the mean (critical) and maximal sizes of clusters

As in previous case, the rate of growth is determined from Eq. (9):

$$\frac{dr}{dt} = \frac{1}{4\pi r^2} j v_m , \tag{39}$$

where j is given by Eq. (38), and j_d and j_v take the magnitudes of left and right parts of inequality (36), respectively:

$$j = D_d \cdot 2\frac{Z_0 q^{1/2}}{2\pi r} q \left(\frac{dC}{dR}\right)_{R=r} + D_v 4\pi r^2 \left(\frac{dC}{dR}\right)_{R=r} , \tag{40}$$

where we take into account that, in a flow j_d, there is $Z = \frac{Z_0 q^{1/2}}{2\pi r}$ (Vengrenovich *et al.*, 2002).

Substituting Eq. (40) in Eq. (39) and taking into account that $\left(\frac{dC}{dR}\right)_{R=r}$ $= \frac{2\sigma v_m}{\mathrm{T}R^*} C_\infty \cdot \frac{1}{r^2}\left(\frac{r}{r_\kappa} - 1\right)$, where σ is the surface energy, C_∞ is the equilibrium concentration of solid solution, R^* is the gas constant, and T is a temperature, one obtains:

$$\frac{dr}{dt} = \frac{1}{4\pi r^4} \frac{2\sigma v_m^2 C_\infty}{R^* \mathrm{T}} \left(D_d 2 \cdot \frac{Z_0 q^{1/2}}{2\pi r} \cdot q + D_v 4\pi r^2 \right) \left(\frac{r}{r_\kappa} - 1\right). \tag{41}$$

Designating, as previously, the shares j_v and j_d in the general flow j as x and $(1-x)$, respectrively, one can represent the rate of growth, Eq. (41), in the form

$$\frac{dr}{dt} = \frac{1}{r^5} \frac{\sigma v_m^2 C_\infty Z_0 q^{3/2} D_d}{2\pi^2 R^* \mathrm{T}} \left(1 + \frac{x}{1-x}\frac{r^3}{r_g^3}\right)\left(\frac{r}{r_\kappa} - 1\right), \tag{42}$$

or:

$$\frac{dr}{dt} = \frac{1}{r^2} \frac{\sigma v_m^2 C_\infty Dv}{R^* \mathrm{T}} \left(\frac{1-x}{x}\frac{r_g^3}{r^3} + 1\right)\left(\frac{r}{r_\kappa} - 1\right). \tag{43}$$

Eq. (42) describes the rate of particle growth for predominant contribution in the general flow of the diffusion matter along dislocations, with the share contribution x of matrix

diffusion; and Eq. (43) describes the rate of growth under matrix diffusion, with the share contribution $(1-x)$ along dislocations.

Eqs. (42) or (43) provide determining the locking point $u_0 = \frac{r_g}{r_k}$, and one finds out from the continuity equation (8), after separation of variables, the specific size distribution function, $f(u)$, where $u = \frac{r}{r_g}$. The ratio $\frac{r_g}{r_\kappa}$, in accordance with (Vengrenovich, 1982), equals:

$$\frac{r_g}{r_\kappa} = \frac{6-3x}{5-3x}. \tag{44}$$

If we let $r = r_g$ in Eq. (42), and the ratio $\frac{r_g}{r_\kappa}$ is replaced by its magnitude from Eq. (44), then after integration one obtains the temporal dependence for maximal

$$r_g = \left(\frac{6A^*}{(5-3x)(1-x)} t \right)^{1/6}, \tag{45}$$

and critical

$$r_\kappa = \left(\frac{6A^*(5-3x)^5}{(6-3x)^6(1-x)} t \right)^{1/6}, \tag{46}$$

particle sizes, where $A^* = \frac{\sigma v_m^2 C_\infty Z_0 q^{3/2} D_d}{2R^* T}$.

Eqs. (45) and (46) describe changing in time the sizes of particles under dislocation-matrix diffusion for predominant contribution of matter diffusion along dislocations. For $x = 0$, that corresponds to the first limiting case, particle growth is limited by diffusion along dislocation:

$$r_g^6 = \frac{6}{5} A^* t, \; r_\kappa^6 = \left(\frac{5}{6} \right)^5 A^* t, \; \frac{r_g}{r_k} = \frac{6}{5}. \tag{47}$$

For that ($x = 0$), the specific size distribution function has a form (Vengrenovich *et al.*, 2002):

$$g'(u) = \frac{u^5 \exp\left(-\frac{0.2}{(1-u)} \right) \exp\left(-0.0287 \tan^{-1}\left(\frac{2u+a}{\sqrt{4b-a^2}} \right) \right) \exp\left(-0.1127 \tan^{-1}\left(\frac{2u+c}{\sqrt{4d-c^2}} \right) \right)}{(1-u)^\alpha \left(u^2 + au + b \right)^\beta \left(u^2 + cu + d \right)^\gamma}, \tag{48}$$

where $a \cong 2.576$, $b \cong 2.394$, $c \cong -0.576$, $d \cong 0.088$, $\alpha \cong 41/15$, $\beta \cong 1.562$, $\gamma \cong 1.572$.
Integrating for the same conditions Eq. (43), one obtains:

$$r_g = \left(\frac{6B^*}{x(5-3x)} t \right)^{1/3}, \tag{49}$$

$$r_{\kappa} = \left(\frac{6B^{*}(5-3x)^{2}}{x(6-3x)^{3}} t \right)^{1/3}, \tag{50}$$

where $B^{*} = \frac{2\sigma v_m C_{\infty} D_v}{R * \mathrm{T}}$.

Another limiting case corresponds to $x = 1$:

$$r_g^3 = \frac{3}{2} B^{*} t, \; r_{\kappa}^3 = \frac{4}{9} B^{*} t, \; \frac{r_g}{r_{\kappa}} = \frac{3}{2}, \tag{51}$$

and the size distribution function is described by the Lifshitz-Slyozov function, Eq. (34):

$$g'(u) = u^2 (1-u)^{-11/3} (u+2)^{-7/3} \exp\left(\frac{1}{1-u} \right).$$

3.2 Size distribution function of clusters

The size distribution function of clusters within the interval $0 \le x \le 1$ is represented, as previously, in the form Eq. (24) (Vengrenovich, 1982), where $g'(u)$ - relative size distribution function, and $u = \frac{r}{r_g}$. From the mass conservation law and disperse phase, Eq. (25), one finds $\varphi(r_g)$, Eq. (26), and, correspondingly,

$$g(u) = Q \cdot g'(u), \tag{52}$$

where $Q = \frac{\mathrm{M}}{\frac{4}{3}\pi\rho \int_0^1 u^3 g'(u) du}$, and ρ – particle density.

If one replaces in the continuity equation (8) $f(r,t)$ and $\dot{r}$ by their magnitudes from Eqs. (24) and (42) (or Eq. (43)) and differentiates u instead of on r and t, then variables in Eq. (8) are separated:

$$\frac{dg'(u)}{g'(u)} = -\frac{4\upsilon_g + 2\frac{\upsilon}{u^3} - \frac{1}{u^2}\frac{d\upsilon}{du}}{u\upsilon_g - \frac{\upsilon}{u^2}} du, \tag{53}$$

where we take into account that $\upsilon = \frac{\dot{r} r^3}{B^{*}}$, $\upsilon_g = \frac{\dot{r}_g r_g^3}{B^{*}}$, $\frac{du}{dr} = \frac{1}{r_g}$, and $\frac{du}{dr_g} = -\frac{u}{r_g}$.

Substituting in Eq. (53) the magnitudes $\upsilon = \left(\frac{1-x}{x}\frac{1}{u^3} + 1 \right)\left(\frac{6-3x}{5-3x} u - 1 \right)$ and $\upsilon_g = \frac{1}{x(5-3x)}$ and decomposing in denominator the second-order polynomial into prime factors, one gets the following form of Eq. (53):

$$\frac{dg'(u)}{g'(u)} = -\frac{4u^6 + u^4\left(6x - 3x^2\right) - 2u^3\left(5x - 3x^2\right) + 4u\left(3x^2 - 9x + 6\right) - 5\left(3x^2 - 8x + 5\right)}{u(1-u)^2\left(u^2 + au + d\right)\left(u^2 + bu + p\right)}du = \tag{54}$$

$$= A\frac{du}{u} + B\frac{du}{1-u} + C\frac{du}{(1-u)^2} + (Du + E)\frac{du}{u^2 + au + d} + (Fu + G)\frac{du}{u^2 + bu + p},$$

where $a = 2.575$; $b = -0.575$; $d = 2.398$; $p = 2.089$.

Integrating Eq. (54), one obtains the analytical form of the relative size distribution function for arbitrary $0 \le x \le 1$:

$$g'(u) = \frac{u^A\left(u^2 + au + d\right)^{\frac{D}{2}}\left(u^2 + bu + p\right)^{\frac{F}{2}}}{(1-u)^B}\exp\left(\frac{C}{1-u}\right)\exp\left(\frac{E - \frac{Da}{2}}{\sqrt{d - \frac{a^2}{4}}}\tan^{-1}\left(\frac{u + \frac{a}{2}}{\sqrt{d - \frac{a^2}{4}}}\right)\right) \times$$

$$\times \exp\left(\frac{G - \frac{Fb}{2}}{\sqrt{p - \frac{b^2}{4}}}\tan^{-1}\left(\frac{u + \frac{b}{2}}{\sqrt{p - \frac{b^2}{4}}}\right)\right), \tag{55}$$

where the coefficients A, B, C, D, E, F, G are found out by matrix solving (Gauss method) the system of seven equations obtained by integrating Eq. (54) ($A = 5; B = 2.731;\ \ C = -0.2;$ $D = -3.117; E = -4.037; F = -3.142;\ \ G = 0.747$) .

3.3 Discussion

Fig. 5 *a* shows the dependences corresponding to the size distribution function, Eq. (52), computed for various magnitudes of x . It is hardly to represent such dependence for $x = 1$ (the Lifshitz-Slyozov distribution) at the same scale; that is why this case is illustrated in other scale at inset.

It is clearly seen that the maxima of curves reached at point u' diminish, as x grows, taking the maximal magnitude for the curve $x = 1$. Magnitude u' itself is determined for the specified x from the following equation:

$$4u^6 + u^4\left(6x - 3x^2\right) - 2u^3\left(5x - 3x^2\right) + 4u\left(3x^2 - 9x + 6\right) - 5\left(3x^2 - 8x + 5\right)\Big|_{u=u'} = 0\,. \tag{56}$$

One can see from Fig. 5 *b*, showing the same dependences normalized by their maxima, that as x grows, as magnitudes u' are shifted to the left (diminish), cf. the inset.

Fig. 6 shows the results of comparison of experimentally obtained histogram with the Liwfitz-Slyozov distribution – (*a*), and the distribution (52) for $x = 0.7$ – (*b*). It is regularly *a priory* assumed (Gaponenko, 1996) that the experimentally obtained histogram shown in Fig. 6 and taken from the paper (Katsikas et al., 1990) that corresponds to the size distribution of nanoclusters of CdS is described by the Lifshitz-Slyozov distribution. However, as one can see from Fig. 6,*b*, the dependence computed by us is narrower, being better fitting a

histogram than the curve in Fig. 6,*a*. It means that formation of quantum dots of *CdS* in process of the Ostwald's ripening obtained by chemical evaporation is realized through mixed diffusion, with 70% share of matrix ($x = 0.7$) and 30% dislocation ($x = 0.3$) diffusion. For that, it is of importance that temporal growth of nanocrystals of *CdS* obeys the cubic law, $\langle r \rangle^3 \sim t$, cf. Eq. (50). It shows that, in first, that the size distribution is formed in process of the Ostwald's ripening, and, secondly, that growth of *CdS* nanocrystals is limited, mainly, by matrix diffusion with the mentioned above share contribution of dislocation diffusion.

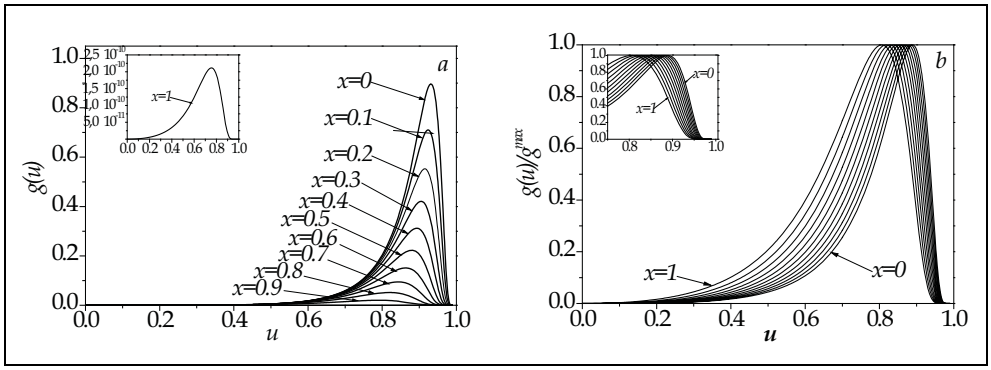


Fig. 5. Size distribution functions, Eq. (52), for various magnitudes of x - *a*; the same distributions normalized by their maxima - *b*

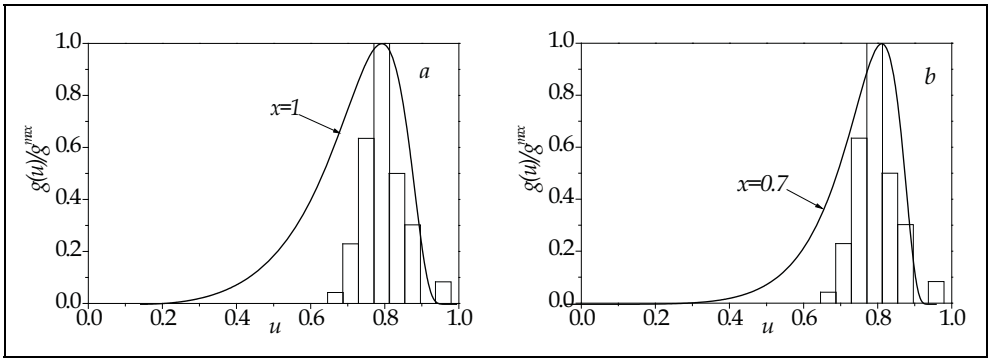


Fig. 6. Comparison with experimentally obtained histogram for nanocrystals of *CdS* (Katsikas *et. al*., 1990) with the theoretical dependence: *a* – the Lifshitz-Slyozov distribution, Eq. (34), *b* – distribution corresponding to Eq. (55) for $x = 0.7$

Let us note that there is the set of quantum dots in semiconductor compounds II-IV obtained by chemical evaporation techniques and having sizes from 1 to 5 nm (Gaponenko, 1996), for which the size distribution function occurs be narrower than one for the Lifshitz-Slyozov distribution.

Similarly to as crystalline gratings of numerous matters are controlled by simultaneous (combined) action of various connection types, the cluster growth goes on under mixed

diffusion, where only one of the types of diffusion can be predominant (matrix, surface, dislocation at the grain boundaries, etc.).

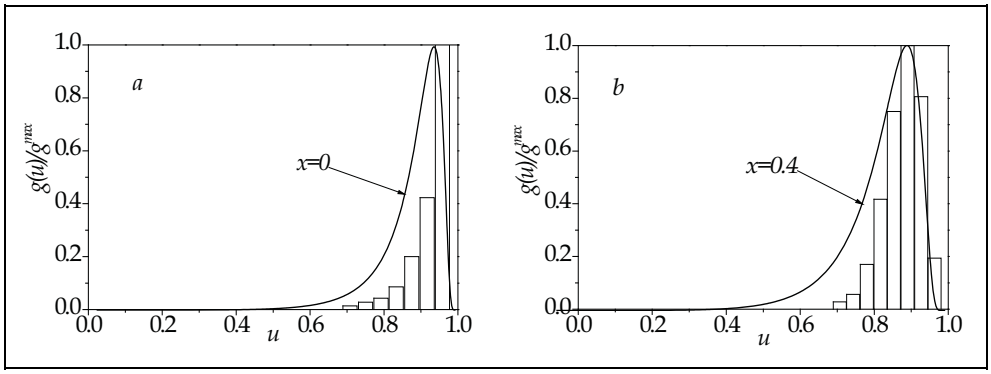


Fig. 7. Example of accidental concurrence of experimentally obtained histogram with the theoretical dependence, Eq. (55), for heterogeneous nucleation of aluminum nanoclusters (Aronin *et al.*, 2001), much earlier than the stage of the Ostwald's ripening comes: *a* – $x = 0$; *b* – $x = 0.4$

Note, the idea of combined action of several mechanisms of diffusion mass transfer has been formulated in several earlier papers (Slyzzov *et al.*, 1978; Sagalovich and Slyozov, 1987). However, the size distribution function for particles coherently connected with the matrix Eq. (55) for combined action of two mechanisms of mass transfer, i.e. diffusion along dislocations and matrix diffusion, has been firstly found by us (Vengrenovich *et al.*, 2007a).

Let us emphasize once more point connected with the study of particle growth under the Ostwald's ripening. It occurs that comparison of the experimentally obtained histograms with the theoretically found dependences does not provide an unambiguous answer the question: What is the mechanism of particle growth? and: is the stage of the Ostwald's ripening occurred? To elucidate these questions, the temporal dependences for a mean particle size, $\langle r \rangle$, are needed.

For example, Fig. 7 shows comparison of experimental histograms for nanoclusters of aluminum obtained by annealing of amorphous alloy $Al_{86}Ni_{11}Yb_3$ (Aronin *et al.*, 2001) with theoretical dependence, Eq. (55), for (*a*) – $x = 0$, and (*b*) – $x = 0.4$. Satisfactory concurrence, however, is accidental. As it is shown in paper (Aronin *et al.*, 2001), the LWS theory is not applicable to this case. Growth of aluminum nanocrystals obeys parabolic dependence $\langle r \rangle \sim t^{1/2}$, rather than to the dependence $\langle r \rangle \sim t^{1/6}$. Histograms in Fig. 7 correspond to heterogeneous nucleation of aluminium clusters that precedes the Ostwald's ripening, which follows much later.

Thus, for estimation of a share (percentage) of the each component, j_d and j_v, in the diffusion flow, one must compare both experimentally obtained histograms with the theoretical dependences and temporal dependences for mean (critical) particle sizes. In the case of metallic alloys strengthened by disperse particles, it enables establishing the mechanism of particle's enlargement, while for quasi-zero-dimension semiconductor structures it makes possible to study, under the Ostwald's ripening, nanoclusters (quantum dots) obtaining by chemical evaporation techniques.

4. Mass transfer between clusters in heterostructures. The generalized Chakraverty-Wagner distribution

The structure and phase dispersion (the particle size distribution function) at the late stages of decay of oversaturated solid solution, i.e. under the stage of the Ostwald's ripening, are determined by the mechanisms of mass transfer between the structure components.

If the particle growth is limited by the coefficient of volume or matrix diffusion D_v, then a mean cluster size, $\langle r \rangle$, changes in time as $t^{1/3}$, and the particle size distribution is governed by the Lifshitz-Slyozov distribution function (Lifshits, Slyozov, 1958, 1961). But if the cluster growth is controlled by the processes at the boundary 'particle-matrix', being governed by the kinetic coefficient β, then $\langle r \rangle$ changes as $t^{1/2}$, and the size distribution function corresponds to the Wagner distribution (Wagner, 1961). In the case of simultaneous action of two mechanisms of growth, dispersion of extractions is described by the generalized LSW distribution (Vengrenovich *et al.,* 2007b).

Generalization of the LSW theory for surface disperse systems, in part, for island films, is of especial interest. This generalization becomes urgent now in connection with development of nanotechnologies and forming nanostructures (Alekhin, 2004; Alfimov *et al.*, 2004; Andrievskii, 2002; Dunaevskii *et al.*, 2003; Dmitriev, Reutov, 2002; Roko, 2002; Gerasimenko, 2002). In part, semiconductor heterostructures with quantum dots obtained under the Stranskii-Kastranov self-organizing process find out numerous practical applications (Bartelt, Evans, 1992; Bartelt *et al.,* 1996; Goldfarb *et al.,* 1997a, 1997b; Joyce *et al.,* 1998; Kamins *et al.,* 1999; Pchelyakov *et al.,* 2000; Ledentsov *et al.,* 1998; Vengrenovich *et al.,* 2001b, 2005, 2006a, 2006b, 2007a).

Chakraverty (Chakraverty, 1967) for the first time applied the LSW theory to describe evolution of structure of discrete films containing of separate islands (clusters) of the form of spherical segments, cf. Fig. 8. Within the Chakraverty model, a film consists of separate cupola-like islands, which are homogeneously (in statistics sense) distributed into oversaturated 'sea' (solution) of atoms absorbed by a substrate, so-called adatoms.

One can see from Fig. 8 that cupola-like clusters are the part of a sphere of radius R_C, with the boundary angle θ. That is why, the radius of base of island, r, length of its perimeter, l, its surface, S, and volume, V, can be expressed through R_C: $r = R_C \sin\theta$, $l = 2\pi R_C \sin\theta$, $S = 4\pi R_C^2 \alpha_2(\theta)$, $V = \frac{4}{3}\pi R_C^3 \alpha_1(\theta)$, where $\alpha_1(\theta) = \frac{2 - 3\cos\theta + \cos^2\theta}{4}$, $\alpha_2(\theta) = \frac{1 - \cos\theta}{2}$ (Hirth, Pound, 1963).

Concentration of adatoms at the cluster base, C_r, is given by the Gibbs-Thomson formula:

$$C_r = C_\infty \exp\left(\Delta P \frac{\upsilon_m}{kT}\right) \approx C_\infty \left(1 + \Delta P \frac{\upsilon_m}{kT}\right), \tag{57}$$

where C_∞ - equilibrium concentration at temperature T, υ_m - volume of adatoms, k - the Boltzmann's constant, ΔP - the Laplasian pressure caused by island surface's curvature. It can be determined by equaling the work necessary for diminishing of an island volume by $d\mathrm{V}$ to the caused by it free energy of island surface:

$$\Delta P d\mathrm{V} = \sigma dS \quad \text{or} \quad \Delta P = \sigma \frac{dS}{d\mathrm{V}} = 2\frac{\sigma}{R_C}\frac{\alpha_2(\theta)}{\alpha_1(\theta)}, \tag{58}$$

where σ - specific magnitude of surface energy.
Taking into account Eq. (58), Eq. (57) can be rewritten in the form:

$$C_r = C_\infty \exp\left(\frac{2\sigma}{R_C}\frac{\upsilon_m}{kT}\frac{\alpha_2(\theta)}{\alpha_1(\theta)}\right) = C_\infty \exp\left(\frac{2\sigma}{r}\frac{\upsilon_m \sin\theta}{kT}\frac{\alpha_2(\theta)}{\alpha_1(\theta)}\right) \approx C_\infty\left(1+\frac{2\sigma}{r}\frac{\upsilon_m \sin\theta}{kT}\frac{\alpha_2(\theta)}{\alpha_1(\theta)}\right). \quad (59)$$

Note, the Gibbs-Thomson formula in the form Eq. (59) has been written for the first time in paper (Vengrenovich *et. al.*, 2008a).

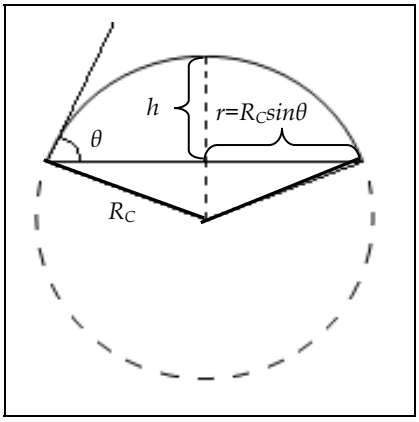


Fig. 8. An island (cluster) in the form of spherical segment as a part of the sphere of radius R_C

Thus, the concentration of adatroms at the boundary 'cluter-substarte' along the line of separation (along the cluster diameter) is determined by the curvature radius of cluster base, r, as it is expected for a plane problem. As the cluster radius diminishes, as the concentration of adatoms at the interface with the cluster must grow. And *vice versa*, as cluster size grows as C_r diminishes. For that, some mean concentration, $\langle C \rangle$, is set in at a substrate that is determined by the critical radius r_k:

$$\langle C \rangle = C_\infty \exp\left(\frac{2\sigma}{r_k}\frac{\upsilon_m \sin\theta}{kT}\frac{\alpha_2(\theta)}{\alpha_1(\theta)}\right) \approx C_\infty\left(1+\frac{2\sigma}{r_k}\frac{\upsilon_m \sin\theta}{kT}\frac{\alpha_2(\theta)}{\alpha_1(\theta)}\right) \quad (60)$$

The clusters for which $C_r > \langle C \rangle$ will dissolve. The clusters for which $C_r < \langle C \rangle$ will grow. So, the clusters of critical size r_k are in equilibrium with a solution of adatoms and radius of such adatoms is determined by Eq. (60):

$$r_k = \frac{\alpha}{\Delta}, \quad (61)$$

where oversaturation is $\Delta = \langle C \rangle - C_\infty$, and $\alpha = \frac{2\sigma C_\infty \upsilon_m}{kT}\sin\theta\frac{\alpha_2(\theta)}{\alpha_1(\theta)}$.

For the diffusion mechanism of growth of cupola-like clusters, the mass transfer between them is realized through surface diffusion under conditions of self-consistent diffusion field (Sagalovich, Slyozov, 1987; Kukushkin, Osipov, 1998) that is characterized by the surface

diffusion coefficient, D_S. Adatoms reaching island perimeters through surface diffusion and overcoming the potential barrier at the interface 'island-substrate', occur at their surfaces. Redistribution of adatoms at cluster surface is made by capillary forces, *viz*. surface tension forces.

In accordance with Wagner, the diffusion growth mechanism with maintenance of island form, i.e. with maintenance of the boundary angle θ is possible, if atoms crossing the interface 'island-substrate' and occurring at their surface in unite time have the time to form chemical connections necessary for reproduction of island matter structure. If it is not so, then adatoms are accumulated near the interface 'island-substrate' with concentration C, that is equal to mean concentration of a solution, $\langle C \rangle$. For that, the process of growth is no more controlled by the surface diffusion coefficient, D_S, but rather by the kinetic coefficient β.

Following to Wagner (Wagner, 1961), the number of adatoms crossing the boundary 'island-substrate' and occurring at the island surface at unite of time is determined as:

$$j_1 = 4\pi R_C^2 \alpha_2(\theta)\beta\langle C\rangle = 4\pi r^2 \frac{\alpha_2(\theta)}{\sin^2\theta}\beta\langle C\rangle, \tag{62}$$

and the number of atoms leaving it at unite of time equals:

$$j_2 = 4\pi r^2 \frac{\alpha_2(\theta)}{\sin^2\theta}\beta C_r, \tag{63}$$

so that the total flow of atoms involved into formation of chemical connection is:

$$j_i = j_1 - j_2 = 4\pi r^2 \frac{\alpha_2(\theta)}{\sin^2\theta}\beta\left(\langle C\rangle - C_r\right), \tag{64}$$

where C_r is determined by Eq. (59).

At the same time, the diffusion flow of adatoms, j_S, to (from) an island is determined by the concentration gradient, $\left(\frac{dC}{dR}\right)_{R=r}$, at the boundary 'island-substrate':

$$j_S = 2\pi r D_S \left(\frac{dC}{dR}\right)_{R=r}. \tag{65}$$

It can be determined by solving the Fick equation that describes concentration of adatoms in the vicinity of isolated island. This equation, within the conditions of stationarity and radial symmetry, takes the form:

$$\frac{1}{R}\frac{d}{dR}\left(RD_S\frac{dC}{dR}\right) = 0, \tag{66}$$

where R is changed within the interval $r \le R \le lr$, $l = 2;3$ (screening distance (Chakraverty, 1967)).

Solution of Eq. (66) can be represented in the form:

$$C(R) = C_1 \ln\frac{R}{r} + C_2, \tag{67}$$

where the constants C_1 and C_2 are determined form the boundary conditions:

$$C(R) = C_r \text{, if } R = r \text{,} \tag{68}$$

$$C(R) = \langle C \rangle \text{, if } R = lr \text{,} \tag{69}$$

from which one obtains:

$$C_1 = \frac{\langle C \rangle - C_r}{\ln l} \text{,} \quad C_2 = C_r \text{.} \tag{70}$$

Thus, the solution of Eq. (67) takes the form:

$$C(R) = \frac{\langle C \rangle - C_r}{\ln l} \ln \frac{R}{r} + C_r \text{.} \tag{71}$$

Knowing $C(R)$, one can determine j_S:

$$j_S = \frac{2\pi D_S}{\ln l} \left(\langle C \rangle - C_r \right) \text{.} \tag{72}$$

At the equilibrium state:

$$j_i = j_S = j \text{.} \tag{73}$$

Thus, the flow j to (from) a cluster can be written as:

$$j = \frac{1}{2} \left(j_i + j_S \right) \text{.} \tag{74}$$

In general case, the flow j equals:

$$j = j_i + j_S \text{.} \tag{75}$$

Thus, the problem of determination of the cluster size distribution function is reduced to accounting the ratio between the flows j_i and j_S in the equation of cluster growth rate.

4.1 Island growth rate

The rate of growth of isolated island (cluster) is determined form the following condition:

$$\frac{d}{dt} \left(\frac{4}{3} \pi R_C^3 \alpha_1(\theta) \right) = \frac{d}{dt} \left(\frac{4}{3} \pi \frac{r^3}{\sin^3 \theta} \alpha_1(\theta) \right) = j \upsilon_m \text{,} \tag{76}$$

where j is given by Eq. (75). Taking into account Eqs. (64) and (72), one finds from Eq. (76) the rate of cluster growth:

$$\frac{dr}{dt} = \frac{1}{4\pi r^2} \frac{\sin^3 \theta}{\alpha_1(\theta)} \upsilon_m \left[4\pi r^2 \frac{\alpha_2(\theta)}{\sin^2(\theta)} \beta \left(\langle C \rangle - C_r \right) + \frac{2\pi D_S}{\ln l} \left(\langle C \rangle - C_r \right) \right] \text{.} \tag{77}$$

Designating the ratio of flows as:

$$\frac{j_S}{j_i} = \frac{x}{1-x}, \tag{78}$$

where $x = j_S/j$ is the contribution of the flow j_S in the total flow j and, correspondingly, $(1-x) = j_i/j$, the rate of growth of islands, Eq. (77), under surface diffusion with the share contribution $(1-x) = j_i/j$ of the part of flow controlled by the kinetic coefficient β, is rewritten in the form:

$$\frac{dr}{dt} = \frac{\sigma C_\infty \upsilon_m^2 D_S}{2kT} \frac{\sin^4\theta\alpha_2(\theta)}{\alpha_1^2(\theta)\ln l} \frac{1}{r^3}\left(\frac{1-x}{x}\frac{r^2}{r_g^2}+1\right)\left(\frac{r}{r_k}-1\right) = \frac{A^*}{r^3}\left(\frac{1-x}{x}\frac{r^2}{r_g^2}+1\right)\left(\frac{r}{r_k}-1\right), \tag{79}$$

where $A^* = \frac{\sigma C_\infty \upsilon_m^2 D_S}{2kT} \frac{\sin^4\theta\alpha_2(\theta)}{\alpha_1^2(\theta)\ln l}$.

For $x = 1$, Eq. (79) takes the following simplified form:

$$\frac{dr}{dt} = \frac{A^*}{r^3}\left(\frac{r}{r_k}-1\right), \tag{80}$$

coinciding with the diffusion rate of growth of islands (Chakraverty, 1967; Eq. (17)).
If the rate of island growth is controlled by the kinetic coefficient β with the share contribution of a flow due to surface diffusion, ($x = j_S/j$), then the rate of growth, Eq. (79), takes the form:

$$\frac{dr}{dt} = \frac{\sigma C_\infty \upsilon_m^2 \beta}{kT} \frac{\sin^2\theta\alpha_2^2(\theta)}{\alpha_1(\theta)} \frac{1}{r}\left(\frac{x}{1-x}\cdot\frac{r_g^2}{r^2}+1\right)\left(\frac{r}{r_k}-1\right) = \frac{B^*}{r}\left(\frac{x}{1-x}\cdot\frac{r_g^2}{r^2}+1\right)\left(\frac{r}{r_k}-1\right), \tag{81}$$

where $B^* = \frac{\sigma C_\infty \upsilon_m^2 \beta}{kT} \frac{\sin^2\theta\alpha_2^2(\theta)}{\alpha_1(\theta)}$.

For $x = 0$, Eq. (81) is rewritten as:

$$\frac{dr}{dt} = \frac{B^*}{r}\left(\frac{r}{r_k}-1\right), \tag{82}$$

that coincides with the equation for the rate of island growth controlled by the kinetic coefficient β (Chakraverty, 1967; Eq. (31)).

4.2 Temporal dependences for critical (r_k) and maximal (r_g) sizes of islands (clusters)

For integrating Eqs. (79) and (81) to determine the temporal dependences of r_k and r_g, it is necessary to determine the magnitudes of the locking point, $u_0 = r_g/r_k$. Its magnitude, in accordance with paper (Vengrenovich, 1982), is found from the condition:

$$\frac{d}{dr}\left(\frac{\dot{r}}{r}\right)\Big|_{r=r_g} = 0, \tag{83}$$

where, for example:

$$\frac{\dot{r}}{r}=\frac{A^*}{r^4}\left(\frac{1-x}{x}\frac{r^2}{r_g^2}+1\right)\left(\frac{r}{r_k}-1\right). \tag{84}$$

By differentiation, one finds:

$$u_0=\frac{r_g}{r_k}=\frac{2x+2}{2x+1}. \tag{85}$$

For $x=0$ (the Wagner mechanism of growth), $r_g/r_k=2$, and for $x=1$ (the diffusion mechanism of growth), $r_g/r_k=4/3$.

Using the magnitude u_o of the locking point, Eq. (85), one can express the specific rate of growth $\dot{r}/r$, Eq. (84), through dimensionless variable, $u=r/r_g$, that enables its representation not schematically, but in the form of a graph for various magnitudes of the parameter x:

$$\upsilon'=\frac{r_g^4}{A^*}\frac{dr}{dt}=\frac{1}{u^4}\left(\frac{1-x}{x}u^2+1\right)\left(\frac{2x+2}{2x+1}u-1\right), \tag{86}$$

where the dimensionless specific rate of growth is $\upsilon'=\frac{r_g^4}{A^*}\frac{dr}{dt}$.

Fig. 9 shows the dependence of υ' on u as a function of x. The role of the locking point consists in that within the LSW theory all solutions, including the size distribution function, are determined for magnitudes u_o alone. It means physically that under the Ostwald's ripening process, the relation between critical and maximal sizes of clusters is always the same, i.e. being constant one.

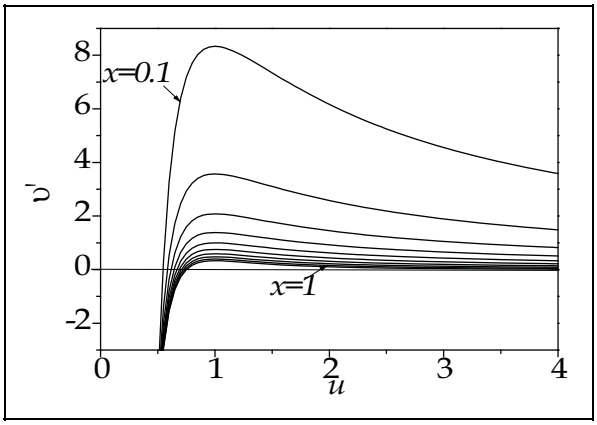


Fig. 9. Dependence of the dimensionless growth rate, υ', on u for various magnitudes of x

For determining r_g and r_k, we use Eqs. (79) and (81). Substituting in Eq. (79) $r=r_g$ and replacing the ratio r_g/r_k by its magnitude (85), one obtains after integrating:

$$r_g^4=4\frac{A^*}{x(2x+1)}t, \tag{87}$$

or:

$$r_k^4 = 4A^* \frac{(2x+1)^3}{x(2x+2)^4} t \,. \tag{88}$$

For $x = 1$, growth of islands is fully controlled by the surface diffusion coefficient (Chakraverty, 1967):

$$r_g^4 = \frac{4}{3} A^* t \,, \;\; r_k^4 = \frac{27}{64} A^* t \,, \;\; \frac{r_g}{r_k} = \frac{4}{3} \,. \tag{89}$$

In the same way, one obtains from Eq. (81):

$$r_g^2 = 2\frac{B^*}{(1-x)(2x+1)} t \,, \; r_k^2 = 2\frac{B^*(2x+1)}{(1-x)(2x+2)^2} t \,. \tag{90}$$

Eq. (90) describes of island growth under conditions controlled by the kinetic coefficient β, with the contribution x of surface diffusion. If $x = 0$, then the growth process is fully controlled by kinetics of crossing the interface 'island-substrate' (Wagner, 1961):

$$r_g^2 = 2B^* t \,, \; r_k^2 = \frac{1}{2} B^* t \,, \; \frac{r_g}{r_k} = 2 \,. \tag{91}$$

4.3 Generalized Chakraverty-Wagner distribution for the case of cupola-like islands (clusters)

As previously, the size distribution function of clusters (islands) within the interval $0 \le x \le 1$ is represented as the product $f(r,t) = \varphi(r_g) g'(u)$, where $g'(u)$ is the relative size distribution of clusters, $u = r/r_g$. The function $\varphi(r_g)$ is determined from the conservation law of disperse phase volume:

$$\Phi = \frac{4}{3}\pi\alpha_1(\theta)\frac{1}{\sin^3\theta}\int_0^{r_g} r^3 f(r,t)\,dr \,. \tag{92}$$

Using Eq. (92), one finds:

$$\varphi(r_g) = \frac{Q}{r_g^4} \,, \tag{93}$$

where:

$$Q = \frac{\Phi}{\frac{4}{3}\pi\alpha_1(\theta)\frac{1}{\sin^3\theta}\int_0^1 u^3 g'(u)\,du} \,. \tag{94}$$

Taking into account Eq. (93), the function $f(r,t)$ is rewritten as:

$$f(r,t) = \frac{1}{r_g^4} Q \cdot g'(u) = \frac{1}{r_g^4} g(u) \,, \tag{95}$$

where the relative size distribution function is:

$$g(u) = Q \cdot g'(u). \tag{96}$$

To determine $g'(u)$, we use the continuity equation (8), substituting in it, instead of $f(r,t)$ and $\dot{r}$, their magnitudes from Eqs. (95) and (81) (or 79)). Under preceding from differentiation on r and t to differentiation on u, the variables are separated, and Eq. (8) takes the form:

$$\frac{dg'(u)}{g'(u)} = -\frac{4\upsilon_g - \frac{1}{u}\frac{d\upsilon}{du} + \frac{\upsilon}{u^2}}{u\upsilon_g - \frac{\upsilon}{u}}du, \tag{97}$$

where $\upsilon = \frac{r\cdot\dot{r}}{B^*} = \left(1 + \frac{x}{1-x}\frac{1}{u^2}\right)\left(\frac{2x+2}{2x+1}u - 1\right)$, $\upsilon_g = \upsilon\big|_{u=1} = \frac{r_g}{B^*}\frac{dr_g}{dt} = \frac{1}{(1-x)(2x+1)}$, $\frac{du}{dr} = \frac{1}{r_g}$, $\frac{du}{dr_g} = -\frac{u}{r_g}$.

Substituting υ, υ_g and $d\upsilon/du$ in Eq. в (97), one obtains the expression:

$$\frac{dg'(u)}{g'(u)} = -\frac{4u^4 - u^2\left(1 + x - 2x^2\right) + 4u\left(x^2 + x\right) - 3x(2x+1)}{u(1-u)^2\left(u^2 + 2ux^2 + 2x^2 + x\right)}du, \tag{98}$$

after integration of which we find $g'(u)$, i.e. the generalized Chakraverty-Wagner distribution for islands of cupola-like form:

$$g'(u) = \frac{u^3\left(u^2 + 2ux^2 + 2x^2 + x\right)^{D/2}}{(1-u)^B}\exp\left(\frac{F - Dx^2}{\sqrt{2x^2 + x - x^4}}\tan^{-1}\left(\frac{u + x^2}{\sqrt{2x^2 + x - x^4}}\right)\right) \times \exp\left(\frac{C}{1-u}\right), \tag{99}$$

where:

$$\begin{cases} B = \dfrac{32x^4 + 16x^3 + 48x^2 + 13x + 5}{A}, \\ C = -\dfrac{12x^2 + 3x + 3}{A}, \\ D = -\dfrac{80x^4 + 40x^3 + 15x^2 + x + 2}{A}, \\ F = -\dfrac{32x^6 + 16x^5 + 54x^4 + 34x^3 + 8x^2}{A}, \\ A = 16x^4 + 8x^3 + 9x^2 + 2x + 1. \end{cases} \tag{100}$$

For $x = 0$: $B = 5$, $C = -3$, $D = -2$, $F = 0$, $A = 1$, and Eq. (99) is transformed into the Wagner distribution (Wagner, 1961):

$$g'(u) = u(1-u)^{-5} \exp\left(-\frac{3}{1-u}\right). \tag{101}$$

For $x = 1$: $A = 36$, $B = 19/6$, $C = -1/2$, $D = -23/6$, $F = -4$, and Eq. (99) corresponds to the Chakraverty distribution (Chakraverty, 1967):

$$g'(u) = \frac{u^3 \exp\left(-\frac{1}{2(1-u)}\right) \exp\left(-\frac{1}{6\sqrt{2}} \tan^{-1}\left(\frac{u+1}{\sqrt{2}}\right)\right)}{(1-u)^{19/6}\left(u^2+2u+3\right)^{23/12}}. \tag{102}$$

Taking into account the volume (mass) conservation law for island condensate, one can find the cluster's relative size distribution function $g(u)$ from Eq. (96).

4.4 Discussion

The dependences shown in Fig. 10 *a* correspond to the size distribution function computed using Eq. (96) for various magnitudes of x. The extreme curves for $x = 0$ and $x = 1$ determine the Chakraverty distribution and the Wagner distributions, respectively (Wagner, 1961; Chakraverty, 1967). All other curves, within interval $0 < x < 1$, describe the size distribution of islands for simultaneous action of the Wagner and diffusion mechanisms of cluster growth (the generalized Chakraverty-Wagner distribution.).

The same dependences normalized by their maxima are shown in Fig. 10 *b*. In such form, being normalized by unity along the coordinate axes, such dependences are easy-to-use for comparison with experimentally obtained histograms.

For the computed family of distributions, see Eq. (96), the magnitude of the locking point changes in accordance with Eq. (85) within the interval $4/3 \le u_0 \le 2$. For $x = 0.5$, one obtains $u_0 = 3/2$, what coincides with similar magnitude for the Lifshitz-Slyozov distribution. At the same time, the curve Eq. (96) for $x = 0.5$ is not the Lifshitz-Slyozov distribution:

$$g(u) = \frac{u^3 \exp\left[-1.084435 \tan^{-1}\left(1.032795u + 0.258199\right)\right] \cdot \exp\left(-\frac{1.2}{1-u}\right)}{(1-u)^{\frac{22}{5}}\left(u^2 + 0{,}5u + 1\right)^{\frac{4}{3}}}. \tag{103}$$

It means that one can not judge on the type of distribution proceeding from the locking point magnitude u_0. It must be considered only as evaluating parameter for choice of the theoretical curve from the family Eq. (96), for comparison with specific experimentally obtained histogram.

Once more important property of the found distribution, Eq. (96), consists in that it can be used not only for comparison with experimentally obtained histograms in the form of distribution of particles of radii r (or diameters d), but also for description of the particle height distribution, h. One can see in Fig. 8 that island height is equal to:

$$h = R_C(1 - \cos\theta) = r\frac{1-\cos\theta}{\sin\theta}, \tag{104}$$

so that $r/r_g = h/h_g = u$.

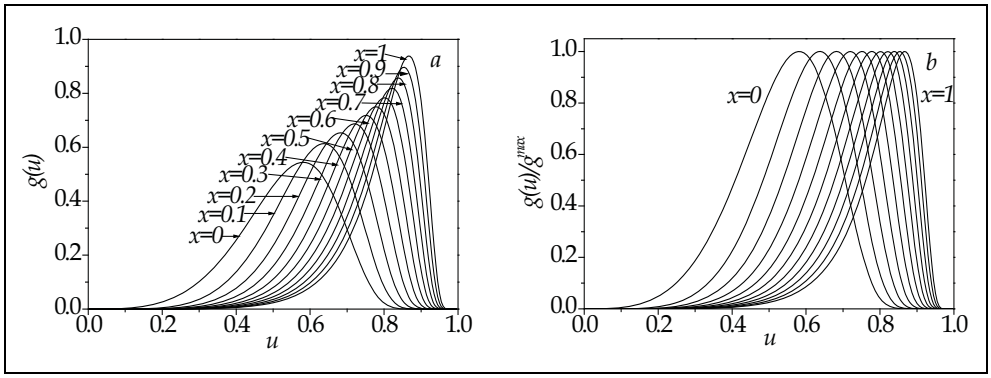


Fig. 10. The generalized Chakraverty-Wagner distribution: *a* – dependences computed for various magnitudes of *x* following Eq. (96); *b* – the same dependences normalized by their maxima

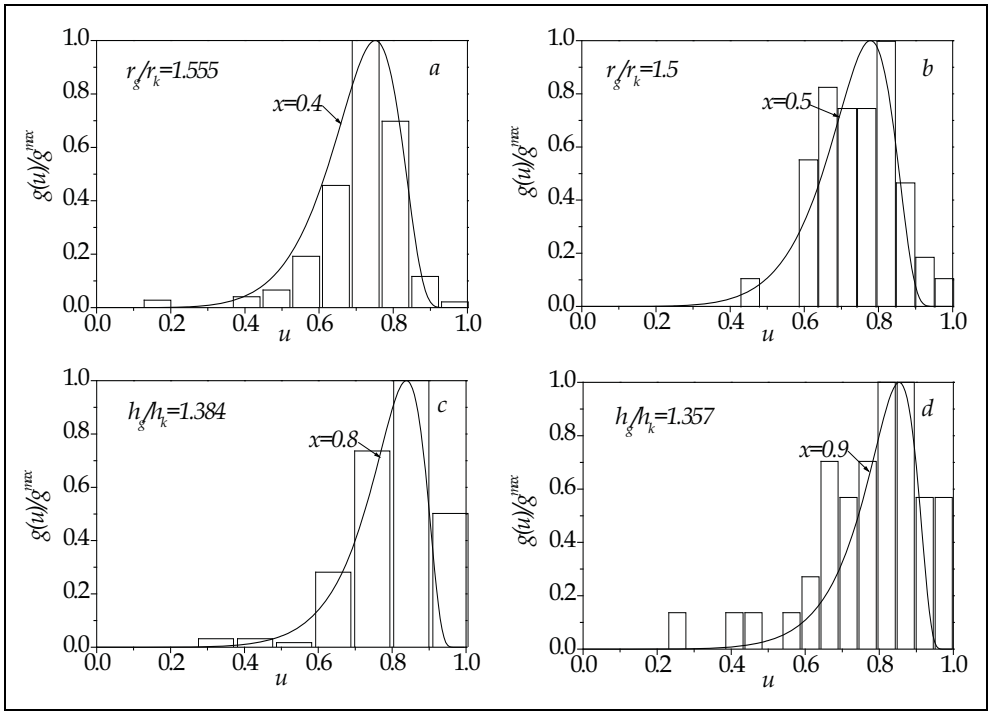


Fig. 11. Comparison of the dependence represented by Eq. (96) with experimentally obtained histograms on diameter, d, and height, h, of nanodots of Mn at various temperatures and thickness of monolayer of Mn : *a* - room temperature, Mn 0.21 ML, $r_g/r_k = 1.555$; *b* - temperature 180°C, $r_g/r_k = 1.5$; *c* - room temperature, Mn 0.21 ML, $h_g/h_k = 1.384$; *d* - temperature 180°C, $h_g/h_k = 1.357$

Fig. 11 shows comparison of experimental histograms of nanodots Mn at substrate Si on diameters, d, (*a* and *b*) and on heights, h, (*c* and *d*), obtained by the molecular beam epitaxy technique at various temperatures, *viz.* at room temperature (fragments *a* and *c*) and at 180˚C (fragments *b* and *d)*, as well as for various thickness of molecular layers of Mn (ML) (De-yong Wang *et. al*., 2006), with theoretical dependence Eq. (96). It is seen from comparison that for experimental distributions on diameters, the contributions of the each of two mechanisms of growth, i.e. Wagner and diffusion ones, are approximately the same, cf. Fig. 11 *a*, $x = 0.4$, and Fig. 11 *b*, $x = 0.5$.

At the same time, the diffusion mechanism occurs to be predominant for the height distribution functions, cf. Fig. 11 *c*, $x = 0.8$, and Fig. 11 *d*, $x = 0.9$. It means that as nanodots of Mn grow, increasing of height leaves behind increasing lateral size d, so that $h/d > 1$. Probably, this circumstance just explains of the form of nanodots of Mn obtained by the authors of paper (De-yong Wang *et al*., 2006).

Fig. 12 shows the results of comparison of the theoretical dependence, cf. Eq. (96), with experimentally obtained histograms of particles of gold obtained at temperature 525°C at silicon substrate $(Au/Si(111))$ - (Fig. 12 *a*), and later, after 180-min isothermal exposure - (Fig. 12 *b*) (Werner *et al*., 2006). Judging by the magnitude of x, particle growth is initially controlled by the kinetic coefficient β (Fig. 12 *a*). But later, the mechanism of growth changes, and after three-hour exposure it becomes predominantly diffusion one (Fig. 12 *b*).

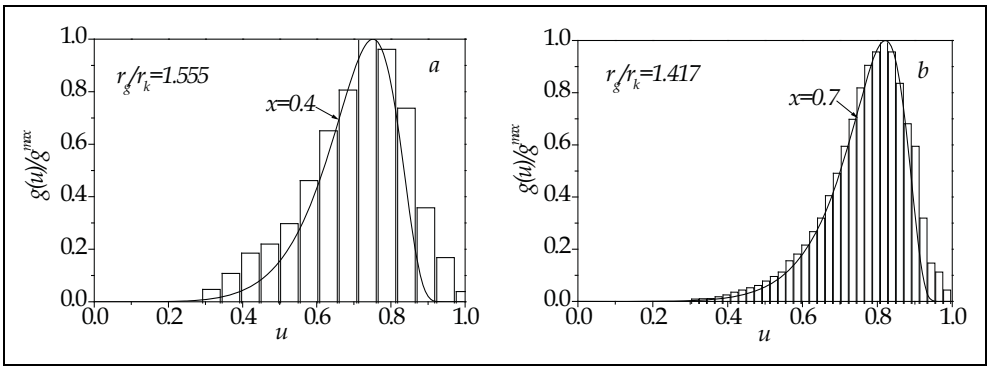


Fig. 12. Comparison of the dependence Eq. (96) with experimentally obtained histograms for particles of *Au* obtained by the molecular beam epitaxy technique for temperature 525°C (*a*) and 180 min later, after isothermal exposure (*b*)

The results of comparison of the theoretical dependence computed for $x = 0.3$ with the experimental histogram for nanoclusters of Ag obtained by the molecular beam epitaxy technique at room temperature at substrate $TiO_2(110)$ (Xiaofeng Lai *et al*., 1999), cf. Fig. 13, also argue in favour of the proposed mechanism of growth.

Thus, the considered examples of comparison of computed and experimentally obtained data leads to the conclusion on the possibility to implement simultaneous action of both mechanisms of growth, i.e. Wagner and diffusion ones. What is more, the situation when both mechanisms of growth co-exist and act in parallel is, to all appearance, more general than separate manifestations of one of two mechanisms considered early by Wagner and Chakraverty.

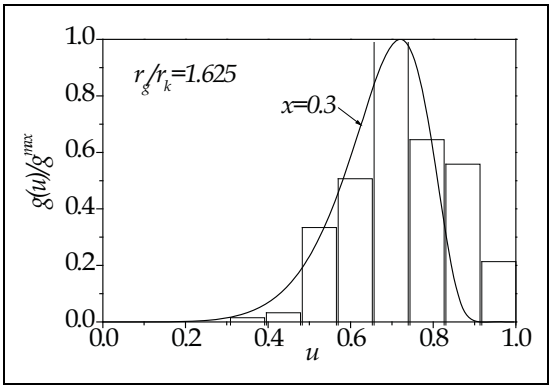


Fig. 13. Comparison of the dependence Eq. (96) with experimental histogram of nanoclusters Ag obtained by the molecular beam epitaxy technique at substrate $TiO_2(110)$ at room temperature

5. Influence of form of nanoclusters in heterostructures on the size distribution function

Obtaining the heterostructures containing quantum dots of specified concentration, form, sizes and homogeneity is connected with considerable experimental difficulties. However, if even such structure has been obtained, its properties can change under the Ostwald's ripening. For that, as it has been shown above, the character of the size distribution function of clusters changes not only as a result of transition from one growth mechanism to another one, but also due to simultaneous action of such mechanisms (Sagalovich & Slyozov, 1987; Vengrenovich *et al*., 2006a, 2007a, 2008a, 2008b). Below we represent the results of investigation of the influence of cluster form on the size distribution function in semiconductor heterosystems with quantum dots. A heterosystem is considered as island film consisting of disk-like islands of cylindrical form, with height h (Fig. 14).

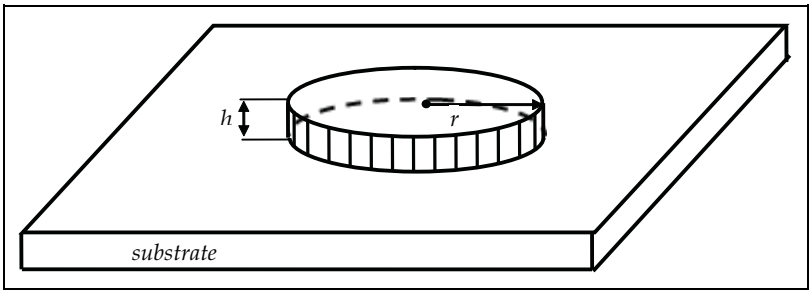


Fig. 14. Disc-like cluster of radius r and constant height h

5.1 Generalized Chakraverty-Wagner distribution for islands (clusters) of cylindrical form ($h = const$)

The problem of determination of the size distribution function is analogous to the above considered problem for clusters of cupola-like form. Modeling the island film by disk-like

islands corresponds to heterostructure with more stable form of hut-clusters (Safonov & Trushin, 2007).
The rate of change of volume of cluster with constant height h (Fig. 14) is determined by the flow j of adatoms to (from) a cluster:

$$\frac{d}{dt}(\pi r^2 h) = j\upsilon_m , \tag{105}$$

where υ_m – adatom volume. From Eq. (105) one obtains:

$$\frac{dr}{dt} = \frac{1}{2\pi rh} j\upsilon_m . \tag{106}$$

Following to (Vengrenovich *et al*., 2008a), the flow j consists of two parts:

$$j = j_S + j_i , \tag{107}$$

where j_S – the part of flow caused by surface diffusion, and j_i – the part of flow of adatoms, which due to overcoming the potential barrier at the interface 'cluster-substrate' fall at cluster surface and, then, take part in formation of chemical connections (the Wagner mechanism of growth).
By definition, the diffusion part of a flow equals:

$$j_S = 2\pi r D_S (\frac{dC}{dR})_{R=r} , \tag{108}$$

where D_S – the surface diffusion coefficient, $(\frac{dC}{dR})_{R=r}$ – concentration gradient at the interface 'cluster-substrate', which can be represented in the form (Chakraverty, 1967; Vengrenovich 1980a, 1980b; Vengrenovich *et al*., 2008a):

$$(\frac{dC}{dR})_{R=r} = \frac{\langle C \rangle - C_r}{\ln l} \cdot \frac{1}{r} , \tag{109}$$

where l determines the distance from an island, $(R = lr)$, at which a mean concentration of adatoms at a substrate, $\langle C \rangle$, is set around separate cluster of radius r ($l = 2, 3$). Taking into account Eq. (109), one can rewrite Eq. (108) in the form:

$$j_S = \frac{2\pi D_S}{\ln l} (\langle C \rangle - C_r) . \tag{110}$$

Concentration of adatoms at the cluster base, C_r, is determined by the Gibbs-Thomson equation:

$$C_r = C_\infty \exp\left(\Delta P \frac{\upsilon_m}{kT} \right) \approx C_\infty (1 + \Delta P \frac{\upsilon_m}{kT}) , \tag{111}$$

where C_∞ – the equilibrium concentration at temperature T, ΔP – the Laplacian pressure caused by island surface curvature, k – the Boltzmann constant. Pressure ΔP, in accordance with (Vengrenovich et al., 2008a), equals:

$$\Delta P = \sigma \frac{dS}{dV} = \sigma \frac{2\pi h dr}{2\pi r h dr} = \frac{\sigma}{r}. \tag{112}$$

Taking into account Eq. (112), C_r can be represented in the form:

$$C_r \approx C_\infty (1 + \frac{\sigma \upsilon_m}{kT} \cdot \frac{1}{r}), \tag{113}$$

where σ – the specific magnitude of surface energy.
A mean concentration of adatoms at surface, $\langle C \rangle$, is determined, by analogy with Eq. (113), by the mean (or critical) cluster size r_k:

$$\langle C \rangle \approx C_\infty (1 + \frac{\sigma \upsilon_m}{kT} \cdot \frac{1}{r_k}). \tag{114}$$

Thus:

$$j_S = \frac{2\pi D_S C_\infty \sigma \upsilon_m}{kT \ln l} (\frac{1}{r_k} - \frac{1}{r}) = \frac{2\pi D_S C_\infty \sigma \upsilon_m}{kT \ln l} \frac{1}{r} (\frac{r}{r_k} - 1). \tag{115}$$

In accordance with Wagner, the number of adatoms occurring in the unite of time at side surface of a cluster $(h = const)$ is determined as:

$$j_1 = 2\pi r h \beta \langle C \rangle, \tag{116}$$

and the number of adatoms leaving a cluster in the unite of time is:

$$j_2 = 2\pi r h \beta C_r, \tag{117}$$

so that the resulting flow of atoms involved into forming chemical connections equals:

$$j_i = j_1 - j_2 = 2\pi r h \beta (\langle C \rangle - C_r) = \frac{2\pi h \beta C_\infty \sigma \upsilon_m}{kT} (\frac{r}{r_k} - 1). \tag{118}$$

Substituting j_S and j_i in Eq. (107), one obtains:

$$j = \frac{2\pi D_S C_\infty \sigma \upsilon_m^2}{kT \ln l} \cdot \frac{1}{r} (\frac{r}{r_k} - 1) + \frac{2\pi h \beta C_\infty \sigma \upsilon_m}{kT} (\frac{r}{r_k} - 1). \tag{119}$$

Substituting Eq. (119) in Eq. (106), one finds out the rate of growth:

$$\frac{dr}{dt} = \frac{1}{2\pi r h} (\frac{2\pi D_S C_\infty \sigma \upsilon_m^2}{kT \ln l} \cdot \frac{1}{r} (\frac{r}{r_k} - 1) + \frac{2\pi h \beta C_\infty \sigma \upsilon_m}{kT} (\frac{r}{r_k} - 1)) \tag{120}$$

For the combined action of two mechanisms of growth, i.e. the diffusion and the Wagner ones, the rate of growth, $\dot{r}$, will be dependent on the ratio of the flows j_S and j_i. Designating, as previously, the shares of flows j_S and j_i in general flow j, as $x = j_S / j$ and $1 - x = j_i / j$, respectively, so that the ratio of them equals:

$$\frac{j_S}{j_i} = \frac{x}{1 - x}, \tag{121}$$

one obtains the formula for the rate of cluster growth under surface diffusion, with the share contribution $(1-x)$ of the flow j_i:

$$\frac{dr}{dt}=\frac{A^*}{r^2}[1+(\frac{1-x}{x})\frac{r}{r_g}](\frac{r}{r_k}-1), \tag{122}$$

or:

$$\frac{dr}{dt}=\frac{B^*}{r}[1+(\frac{x}{1-x})\frac{r_g}{r}](\frac{r}{r_k}-1), \tag{123}$$

that corresponds to the Wagner mechanism of cluster growth with the share contribution x of the diffusion flow j_S, where $A^*=\frac{D_S C_\infty \sigma \upsilon_m^2}{hkT\ln l}$, $B^*=\frac{\beta C_\infty \sigma \upsilon_m^2}{kT}$.

Solving jointly Eq. (122) (or Eq. (123)) and Eq.(8) and applying the method derived in paper (Vengrenovich, 1982), one finds out the generalized relative size distribution function, $g'(u)$, for disk-like clusters corresponding to the combined action of two mechanisms of growth, i.e. the Wagner and the diffusion ones (Vengrenovich *et al*., 2010):

$$g'(u)=u^2(1-u)^{-B}\left(u+x^2+x\right)^D\exp(\frac{C}{1-u}), \tag{124}$$

where:

$$\begin{cases} B=\dfrac{2x^4+4x^3+10x^2+8x+4}{A}, \\ C=-\dfrac{2x^2+2x+2}{A}, \\ D=-\dfrac{3x^4+6x^3+5x^2+2x+1}{A}, \\ A=x^4+2x^3+3x^2+2x+1. \end{cases}, \tag{125}$$

For $x=1$, $B=28/9$, $D=-17/9$, $C=-2/3$, and Eq. (124) corresponds to the distribution obtained in paper (Vengrenovich, 1980):

$$g(u)'=u^2(1-u)^{-28/9}(u+2)^{-17/9}\exp(-\frac{2/3}{1-u}). \tag{126}$$

For $x=0$, $B=4$, $D=-1$, $C=-2$, and Eq. (124) turns into the Wagner distribution (Chakraverty, 1967; Vengrenovich, 1980a, 1980b):

$$g'(u)=u(1-u)^{-4}\exp(-\frac{2}{1-u}). \tag{127}$$

However, for graphic representation of the size distribution function one must carry out computations following equation that is analogous to Eq. (28):

$$g(u)=Q\cdot g'(u), \tag{128}$$

where $Q = \dfrac{\Phi}{\pi h \int_0^1 u^2 g'(u)\,du}$, Φ – the volume (mass) of disperse phase in the form of clusters.

5.2 Discussion

The dependences shown in Fig. 15,*a* correspond to the size distribution function Eq. (128) computed for various magnitudes of x. The limiting curves, for $x = 0$ and $x = 1$, correspond to the Wagner distribution (Wagner, 1961) and to the distribution obtained in papers (Vengrenovich, 1980a, 1980b), respectively. All other distributions within the interval $0 \le x < 1$ describe the size distribution functions of clusters for the combined action of the Wagner and the diffusion mechanisms of growth. The same dependences normalized by their maxima are shown in Fig.15,*b*.

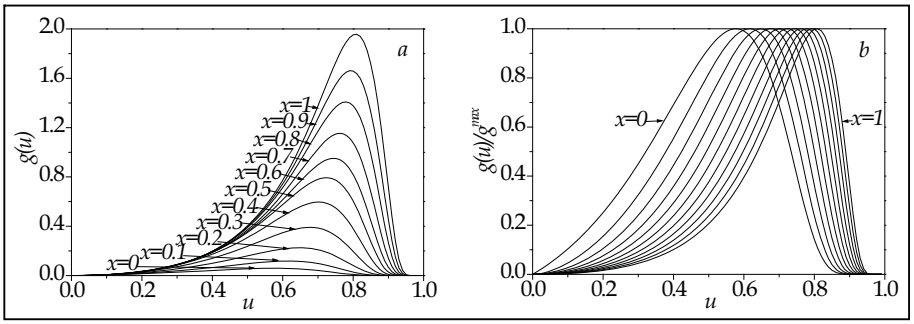


Fig. 15. Functions $g(u)$ (*a*) and $\left(g(u)/g^{\max}\right)$ (*b*) computed following Eq. (128)

Fig. 16 illustrates comparison of experimental histogram of nanodots Ge/SiO_2 (Kan *et al.*, 2005), obtained by evaporating technique with following thermal annealing, with the theoretical dependence, Eq. (128), for $x = 0.7$. A mean size of clusters is 5.6 nm. One can see satisfactory agreement of the theory and experimental data.

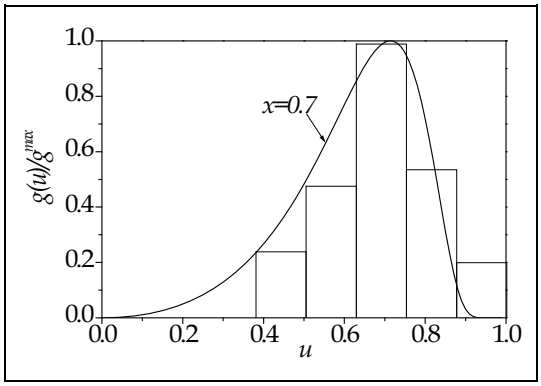


Fig. 16. Comparison of the dependence Eq. (128) with experimental histogram of nanodots Ge at substrate SiO2 obtained by evaporating with following thermal annealing (Kan et al., 2005)

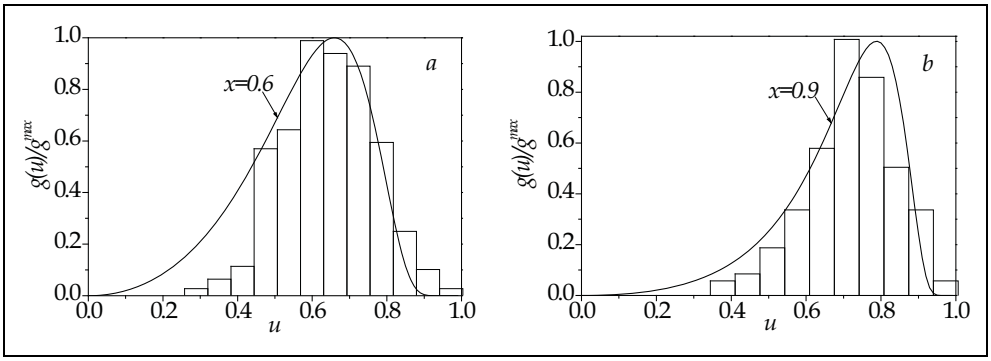


Fig. 17. Comparison of dependence (128) with experimental histograms Ge at substrate Si obtained by molecular beam epitaxy with one (*a*) and two (*b*) layers of nano-clusters Ge (Yakimov *et al*., 2007)

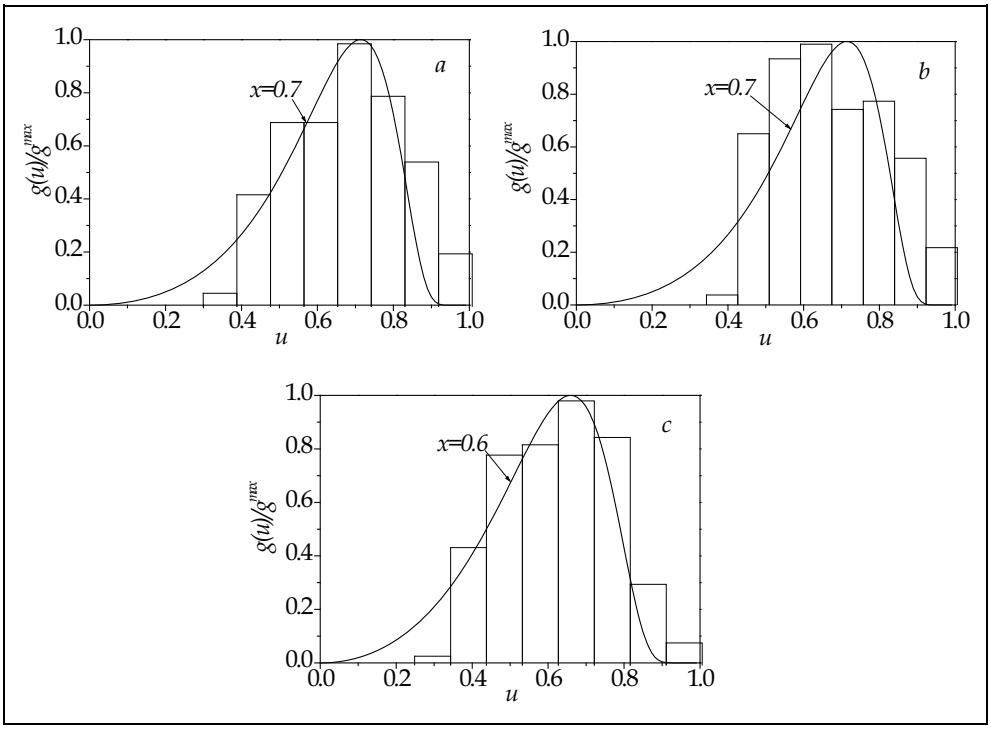


Fig. 18. Comparison of dependence (128) with experimental histograms Co at Si_3N_4 obtained by evaporating at room temperature: (*a*) 0.1 ML Co, (*b*) 0.17 ML Co, (*c*) 0.36 ML Co (Shangjr Gwo *et al*., 2003)

In other case that is illustrated in Fig. 17, the theoretical dependence Eq. (128) is compared with experimental histograms Ge/Si(001) obtained by the molecular-beam epitaxy

technique at temperature 500ºC (Yakimov *et al*., 2007). The experimentally obtained histogram in Fig. 17,*a* corresponds to one layer of nanoclusters of Ge of a main size ~10.4 nm. One can see that for $x = 0.6$ theoretical results are well fitting the experimental data. For two layers of nanoclusters (with a mean size ~10.7 nm), cf. Fig. 17,*b*, ripening of nanoclusters is almost entirely determined by surface diffusion. The diffusion flow j_S constitutes about 90% of the total flow j $\left(j_S = 0.9j\right)$.

It is of especial interest from the theoretical point of view to compare the computed dependences and experimentally obtained histograms illustrated in Fig. 18 (Shangjr Gwo *et al*., 2003). Nanoclusters of Co at Si_3N_4 substrate were obtained by applying the evaporation technique at room temperature with rate (0.3-1.2) ML/min. Histograms shown in Fig. 18 correspond to the following conditions: *a*) 0.1 ML Co; *b*) 0.17 ML Co; c) 0.36 ML Co.

As opposed to heterostructures Ge/Si (001) and Ge/ SiO_2 on the base of quantum dots of Ge, which are widely used in optoelectronics and microelectronics, Co is not semiconductor, and the system Co/Si_3N_4 is the model one for investigation of regularities of forming defect-free nanoclusters.

However, one can see from Figs. 16, 17, and 18 that the regularities of the Ostwald's ripening are the same both for the clusters of semiconductor, Ge, and for metallic clusters of Co. In both cases, irrespectively of metallic or semiconductor nature of clusters, ripening of them is governed by the combined mechanism of growth, i.e. the diffusion and the Wagner's ones, with predomination, in the resulting flow, of the flow j_S due to surface diffusion. It proves generality of the considered by us mechanism of cluster ripening, when the rate of growth of them is determined by the ratio of the diffusion flow, j_S, to the flow j_i through the interface 'cluster-substrate'.

6. Mass transfer between clusters under dislocation-surface diffusion. Size distribution function

Obtaining nanocrystals meeting the requirements raised to quantum dots by applying the conventional techniques, such as selective etching, growth at profiled substrate, chemical evaporation, condensation in glass matrices, crystallization under ultrahigh rate of cooling or annealing of amorphous matrices has not led to desirable results (Ledentsov *et al*., 1998; Pchelyakov *et al*., 2000). And only under the process of self-organization in semiconductor heteroepitaxial systems it occurs possible to form ideal heterostructures with quantum dots.

The technique of heteroepitaxial growing in the Stranski-Kastranov regime (Krastanow & Stranski, 1937) is the most widely used for obtaining quantum dots. In this case, layer-wise growth of a film is replaced, due to self-organization phenomena, by nucleation and following development of nanostructures in form of volume (3D) islands (Bimberg & Shchukin, 1999; Kern & Müller, 1998; Mo *et al.,* 1990). Islands with spatial limitation of charge carriers in all three directions are referred to as quantum dots. Quantum dots obtained in such a way have perfect crystalline structure, high quantum efficiency of radiation recombination and are characterized by enough high homogeneity in size (Aleksandrov *et al.,* 1974; Leonard *et al*., 1993; Moison *et al*., 1994; Ledentsov *et al*., 1996a, 1996b). Sizes of quantum dots can vary from several nanometers to several hundred nanometers. For example, size of quantum dots in heteroystems Ge-Si and InAs-GaAs lies within the interval from 10 nm to 100 nm, with concentration $10^{10} \div 10^{11}$ cm $^{-2}$.

Much prominence is given in the literature to the size distribution function of islands, while this parameter of a system of quantum dots is of high importance in practical applications

(Bartelt *et al*., 1996; Goldfarb *et al*., 1997a, 1997b; Joyce *et al.,* 1998; Kamins *et al*., 1999; Ivanov-Omski *et al*., 2004; Antonov *et al*., 2005). In part, changing the form and sizes of islands, one can control their energy spectrum that is of great importance for practical applications of them. As the size distribution function becomes more homogeneous, as (for other equivalent conditions) the system of quantum dots becomes more attractive from the practical point of view.

Homogeneity of the size distribution function can be conveniently characterized by root-mean-square (*rms*) deviation, $\sigma' = \sqrt{D}$, where D – dispersion. As the size distribution function becomes narrower, as σ' decreases. In this respect, the best size distribution functions have been obtained for island of germanium into heterosystem Ge/Si(001), where $\sigma' < 10\%$ (Jian-hong Zhu *et al*., 1998).

Theoretical distributions corresponding to such magnitudes of dispersion D (or associated magnitudes of *rms*) have been obtained in papers (Vengrenovich *et al*., 2001b, 2005) in assumption that the main factor determining the form of the size distribution function of island film at later stages is the Ostwald's ripening. Computations have been carried out within the LSW theory, in assumption that dislocation diffusion is the limiting factor of the Ostwald's ripening. For that, the dislocation mechanism of growth of islands under the Ostwald's ripening is possible, if the flow of matter due to dislocation diffusion much exceeds the flow due to surface diffusion, i.e.

$$D_s^{(d)} Zd \left(\frac{dC}{dR} \right)_{R=r} >> D_s 2\pi r \left(\frac{dC}{dR} \right)_{R=r} \tag{129}$$

where $D_s^{(d)}$ – the diffusion coefficient along dislocation grooves, D_s – the surface diffusion coefficient, $\left(\frac{dC}{dR} \right)_{R=r}$ – the concentration gradient at island surface, d – the width of dislocation groove, $d = 2\sqrt{2q/\pi}$, $b^2 \le q \le 60b^2$, where b – the Burgers vector, Z – the number of dislocation lines ending at the island base of radius r $\left(Z \equiv const\right)$. For simplifying the computations, islands are considered as disk-like ones, with constant height h (Vengrenovich *et al*., 2001b). General case, when both h and r are changed, is considered in paper (Vengrenovich *et al*., 2005).

Eq. (129) sets limitations on island sizes, which grow due to dislocation diffusion:

$$r << \frac{Zd}{2\pi} \frac{D_s^{(d)}}{D_s} . \tag{130}$$

If the condition Eq. (130) is violated, one must take into account in the resulting flow of matter, beside of the flow due to dislocation diffusion, the flow component caused by surface diffusion.

Under dislocation-surface diffusion one has:

$$j = j_d + j_s , \tag{131}$$

where j_d – the flow to a particle due to diffusion along dislocations, j_s – the flow due to surface diffusion, j_d and j_s are determined by the left and the right sides of Eq. (129), respectively.

The rate of growth of isolated island under condition $h = const$ is determined from equation:

$$\frac{d}{dt}\left(\pi r^2 h\right) = j v_m . \tag{132}$$

Substitution Eq. (131) in Eq. (132) and taking into account the magnitudes of j_d and j_s, as well as of the concentration gradient at the island boundary, one obtains:

$$\frac{dr}{dt} = \frac{\sigma\ v_m^2 C_\infty}{2\pi hkT \ln l}\frac{1}{r^2}\left(D_s^{(d)} Zd\frac{1}{r} + 2\pi D_s\right)\left(\frac{r}{r_k} - 1\right). \tag{133}$$

Taking into account the ratio of flows,

$$x = \frac{j_s}{j},\ 1 - x = \frac{j_d}{j},\ \frac{j_d}{j_s} = \frac{1-x}{x}, \tag{134}$$

one can write Eq. (133) in the form:

$$\frac{dr}{dt} = \frac{\sigma v_m^2 C_\infty D_s^{(d)} Zd}{\pi hkT \ln l}\frac{1}{r^3}\left(\frac{x}{1-x}\frac{r}{r_g} + 1\right)\left(\frac{r}{r_k} - 1\right), \tag{135}$$

or:

$$\frac{dr}{dt} = \frac{\sigma v_m^2 C_\infty D_s}{hkT \ln l}\frac{1}{r^2}\left(\frac{1-x}{x}\frac{r_g}{r} + 1\right)\left(\frac{r}{r_k} - 1\right). \tag{136}$$

Eqs. (135) and (136) describe the rate of growth of clusters under dislocation and surface diffusion with contributions (x) and ($1-x$) corresponding to the flows of them.
Taking into account Eqs. (135) and (136) for the rate of growth and performing computations following the algorithm introduced in paper (Vengrenovich, 1982), one can represent the relative size distribution function of clusters, under assumption that mass transfer between clusters is realized due to dislocation-surface diffusion, in the form:

$$g'(u) = \frac{u^3 (u^2 + bu + c)^{\frac{D}{2}}}{(u-1)^K}\exp\left(\frac{F}{u-1}\right) \times \exp\left(\frac{\frac{E - Db}{2}}{\sqrt{c - \frac{b^2}{4}}}\tan^{-1}\left(\frac{u + b/2}{\sqrt{c - b^2/4}}\right)\right), \tag{137}$$

Where

$$\begin{cases} D = \dfrac{3c^2 + \left(x^2 - 4x + 6b - 6\right)c + 6b^2 + \left(4x^2 - 16x + 14\right)b + 7x^2 - 28x + 19}{c^2 + (b+1)2c + b^2 + 2b + 1}, \\ E = \dfrac{(3-D)c + (D-3)b^2 + (2b+1)D + x^2 - 4x - 3}{2 + b}, \\ F = D(b+1) - 3b - E, \\ K = 6 - D. \end{cases} \tag{138}$$

6.1 Comparison with experimental data

Fig. 19 *a* illustrates the family of distributions computed following Eq. (137) with the step $\Delta x = 0.1$ for magnitudes of x between zero and unity. One can see that as magnitude of x increases, as the maxima of the distributions decreases, and the magnitudes of u' where $g(u')$ reaches maximum are shifted to the left, in direction of decreasing u. This shift is clearly observable in Fig. 19 *b*, where the same distributions normalized by their maxima are shown, so that $g^{\max} \equiv g(u')$. For that, the magnitudes of u' are determined from the following equation:

$$3u^4 - (x^2 - 4x)u^2 + (x^2 - 4x + 2)4u^2 - 3x^2 + 12x - 9\Big|_{u=u'} = 0 \,. \tag{139}$$

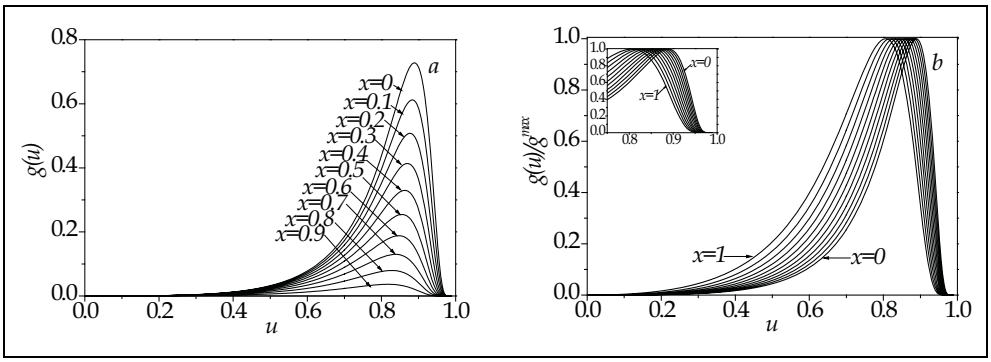


Fig. 19. Size distribution functions computed with the step $\Delta x = 0.1$ (*a*); the same distributions, normalized by their maxima (enlarged version is in the inset), where $g^{\max} \equiv g(u')$ (*b*).

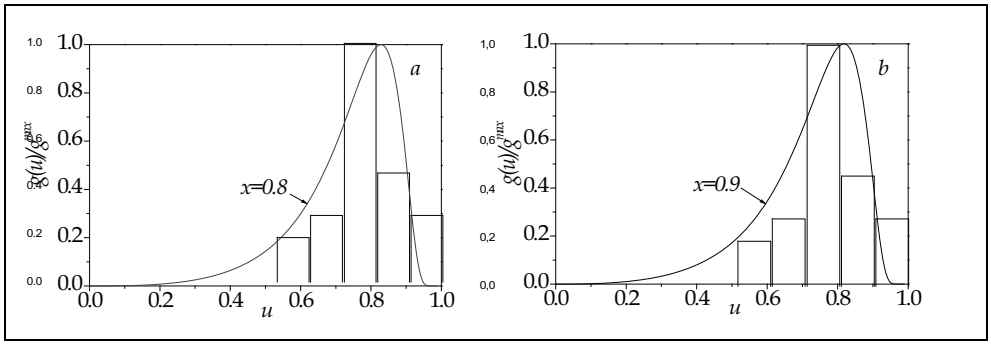


Fig. 20. Comparison with experiment (Neizvestnii *et al.*, 2001) $x = 0.8$ (*a*), $x = 0.9$ (*b*).

It must be noted that in the most cases experimental histograms are obtained as the dependences of the number of islands (share of islands) at the unit area on island's height, h. Theoretically, the choice of variable is arbitrary. For constant rate of change of island volume, it is of no importance, either r or h variable is constant. That is why, the

distributions shown in Fig. 19 can be used also for comparison with experimentally obtained histograms, when the island height, h, is constant.
One of such comparisons is illustrated in Fig. 20 (a – $x = 0.8$, b – $x = 0.9$). Experimentally obtained histogram normalized by unity on axes $u\left(h/h_g\right)$ and $g(u)/g^{\max}$ corresponds to the height (on h) distribution function in (Ge/ZnSe) (Neizvestnii *et al.*, 2001).

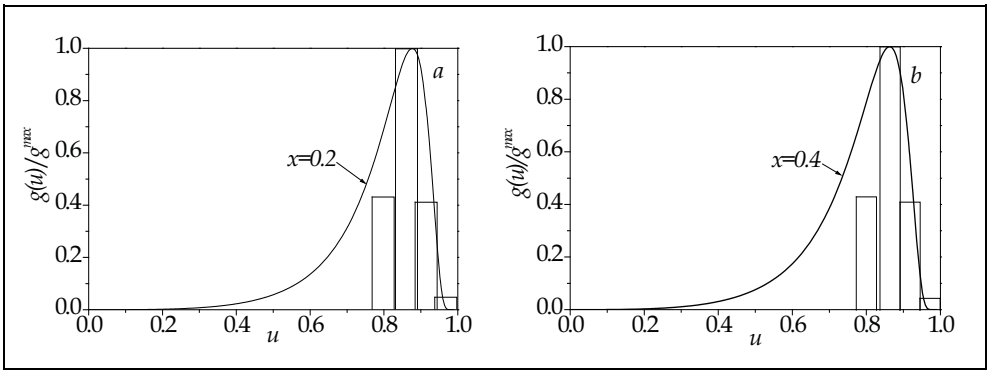


Fig. 21. Comparison of the experimentally obtained histograms with theoretically computed dependences (Vostokov *et al.*, 2000) $x = 0.2$ (*a*), $x = 0.4$ (*b*)

In Fig. 21, the experimentally obtained histogram normalized in the same manner as in previous case, corresponds to the height distribution of islands of germanium (Ge/Si (001)) for the quantity of fall out of germanium 5.5 monolayers ($d_{Ge} = 5.5ML$) (Vostokov *et al.*, 2000). Theoretical curves have been computed for a – $x = 0.2$, and b – $x = 0.4$. One can see that as x increases, as discrepancy between the experimentally obtained histogram and theoretically computed dependences increases also.

7. Conclusions

We have developed the theory of the Ostwald's ripening, taking into account not only mass transfer between clusters due to diffusion (volume, surface, dislocation), but also the kinetics of mass transfer through the interface 'cluster-matrix' ('cluster-substrate') determining the formation of chemical connections at cluster surface (the Wagner mechanism of cluster growth).
Within the developed by us theory, diffusion and kinetics of mass transfer through the interface 'cluster-matrix' are taken into account as the corresponding flows, $j_V\,(j_S)$ and j_i, in the resulting flow to (from) a cluster: $j = j_V\,(j_S) + j_i$. The contribution of the each mechanism of mass transfer in the resulting flow, j, is represented as the ratio of the partial flows: $x = \frac{j_V}{j}\left(\frac{j_S}{j}\right)$ and $1 - x = \frac{j_i}{j}$. Taking into account both diffusion and kinetics of mass transfer through interface of two structural components means that one can not neglect any of the components of flow j, both $j_V\,(j_S)$ and j_i. It corresponds to the model of cluster ripening, in accordance with which growth of them is governed by two mechanisms, i.e. by the Wagner and by the diffusion ones. Within the framework of this model, the size

distribution function of clusters is described by the generalized Lifshitz-Slyozov-Wagner distribution (alloys, nanocomposites as nc CdS / polimer (Savchuk *et al*., 2010a, 2010b, 2010c) or the generalized Chakraverty-Wagner distribution (island films, heterostructures with quantum dots, etc.)

If in the resulting flow j the component $j_i << j_V$, it can lead to new mechanism of cluster growth under dislocation-matrix or dislocation-surface diffusion, for the each of which the specific size distribution function and the corresponding temporal dependences of $\langle r \rangle$ and r_g are intrinsic.

Comparison of the theoretically computed size distribution functions with experimentally obtained histograms leads to the following two main conclusions.

1. The introduced model of cluster ripening under simultaneous (combined) action of both the diffuse mechanism and the Wagner one is proved experimentally. Other of the considered models is also finds out experimental proof, *viz.* the case when one neglects the Wagner mechanism of growth and cluster ripening results from mixed dislocation-matrix and dislocation-surface diffusion. Thus, it is the most likelihood that, in practice, cluster growth follows to not only one isolated of the considered early mechanisms of growth, i.e. the diffusion mechanism or the Wagner one, but rather to the mixed (combined) mechanism, when two mentioned limiting mechanisms act together.

It also follows from the results of comparison of the computed and experimental data, that cluster growth under mixed (combined) dislocation-matrix or dislocation-surface diffusion is most probable than cluster growth under any of two mentioned mechanisms, if isolated.

2. In connection with intense development of nanotechnologies and related techniques for generating of nanostructures, the problem arises: in what framework is the LSW theory applied to analysis of nanosystems containing nanoclusters. The final answer on this question is now absent. Also, the main question concerning stability of nanosystems in respect to the Ostwald's ripening leaves opened. Nevertheless, it follows from the represented by us results of comparison of theoretical and experimental data, that in many cases the experimentally obtained histograms built for nanoparticles (nanoclusters) by many authors for various nanosystems are quite satisfactory fitted by the computed by us theoretical distributions (the generalized Lifshitz-Slyozov-Wagner distribution, the generalized Chakraverty-Wagner distribution etc.). In means that the developed by us LSW theory can be, in principle, be used for analysis of phase and structural transformations in nanosystems with nanophases. Of course, derived by us approach requires further investigations, both theoretical and experimental.

8. Acknowledgement

This investigation has been carried out under supporting the Ministry of Education and Science of Ukraine, grant No0110 U000190.

9. References

Alechin A.P. (2004). Structural organization of a matter at surface in nanotechnology – a way to nanotechnology. *Russian Usp. Mod. Radioelectr.*, V. 5, (2004), pp. 118-122

Aleksandrov L.N., Lovyagin R.N., Pchelyakov O.P., Stenin S.I. (1974). Heteroepitaxy of germanium thin films on silicon by ion sputtering. *J. Cryst., Growth*, V. 24-25, (1974), pp. 298-301

Alfimov S.M., Bykov V.A., Grebennikov E.P., Zheludeva S.I., Malzev P.P., Petrunin V.F., Chapligin Yu.A. (2004). Development of R&D in nanotechnologies in Russia. *Microsystem Technique,* V. 8, (2004), pp. 2-8

Andrievskiy R.A. (2002). Nanomaterials: the concept and modern problems. *Russian Chem. J.*, V. 46, (2002), pp. (50-56)

Antonov A.V., Gaponova D.M., Danilzev V.M., Drozdov M.N., Moldavskaya L.D., Murel A.V., Tulovchikov V.S., Shashkin V.I. (2005). Heterostructures InGaAs/GaAs with quantum dots for IR photodetectors within the region 3-5 μm. *Russian Phys. Semicond.*, V.39, No. 1. pp. 96-99

Ardell A.J. (1972). On the coarsening of grain boundary precipitates. *Acta Metall*, Vol. 20, (1972), pp. 602-609

Aronin A.S., Abrosimova U.Ye., Kiryanov Yu.V. (2001). Formation and structure of nanocrystals in alloy $Al_{86}Ni_{11}Yb_3$. *Russian Phys. Solid State,* V. 43, No. 11, (2001), pp. 1925-1933

Bartelt M.C., Evans J.W. (1992). Scaling analysis of diffusion-mediated island growth in surface adsorption processes. *Phys. Rev. B,* V. 46, No. 19, (1992), pp. 12675-12687

Bartelt N.C., Theis W., Tromp R.M. (1996). Ostwald ripening of two-dimensional islands on Si(001). *Phys. Rev. B,* V. 54, No. 16, (1996), pp. 11741-11751

Chakraverty B.K. (1967). Grain size distribution in thin films. I. Conservative systems. *J. Phys. Chem. Solid.,* V. 28, (1967), pp. 2401-2412

De-yong Wang, Li-jun Chen, Wei He, Qing-feng Zhan and Zhao-hua Cheng. (2006). Preferential arrangement of uniform Mn nanodots on Si(111)-7 × 7 surface. *J. Physics. D, Applied Physics* V. 39, No. 2, (2006), pp. 347-350

Dunaevskiy M.S., Krasilnik Z.F., Lobanov D.N., Novikov A.V., Titkov A.N., Laiho R. (2003). Vizualization of tangled nanoislands of GeSi vi silocon structures by atom-force technique at knocks. *Russian Phys. Semicond.*, V. 37, (2003), pp. 692-699

Gaponenko S.V. (1996). Optical processes in semiconductor nanocrystals (quantum dots). Review. *Russian Phys. Semicond.*, V. 30, No. 4, (1996), pp. 577-619

Gerasimenko N.N. (2002). Nanoscale structures in implanted semiconductors. *Rusian Chem. J.*, V. 46, (2002), pp. 30-41

Goldfarb I., Hayden P.T., Owen J.H.G., Briggs G.A.D. (1997a) Nucleation of "Hut" Pits and Clusters during Gas-Source Molecular-Beam Epitaxy of Ge/Si(001) in *In Situ* Scanning Tunneling Microscopy. *Phys. Rev. Lett,* V. 78, No. 20, (1997), pp. 3959-3962

Goldfarb I., Hayden P.T., Owen J.H.G., Briggs G.A.D. (1997b). Competing growth mechanisms of Ge/Si(001) coherent clusters. *Phys. Rev. B,* V. 56, (1997), pp. 10459-10468

Hirth J. P., Pound G. M. (1963). Condensation and Evaporation, Nucleation und Growth Kinetics; Band 11 der Serie "Progress in Material Science", herausgegeben von Bruce Chalmers, Pergamon Press, Oxford-London-Paris-Frankfurt; 190 Seiten

Ivanov-Omsky V.I., Kolobov A.V., Lodygin A.B., Yastrebov S.G. (2004). Size distribution of clusters of cobalt in amorphous carbon matrix. *Russian Phys. Semicond.*, V. 38, No. 12 (2004), pp. 1463-1465

Jian-hong Zhu, Brunner K., Abstreiter G. (1998). Two-dimensional ordering of self-assembled Ge islands on vicinal Si(001) surfaces with regular ripples. *Appl. Phys. Lett*, V. 73, No. 5, (1998), pp. 620-622

Joyce B.A., Vvedensky D.D., Avery A.R., Belk J.G., Dobbs H.T., Jones T.S. (1998). Nucleation mechanisms during MBE growth of lattice-matched and strained III–V compound films. *Appl. Surf. Sci*, V. 130-132, (1998), pp. 357-366

Kamins T.I., Medeiros-Ribeiro G., Ohlberg D.A.A., Stanley Williams R. (1999). Evolution of Ge islands on Si(001) during annealing. *J. Appl. Phys,* V. 85, No. 2, (1999), pp. 1159-1171

Kan E. W. H., Koh B. H., Choi W. K., Chim W. K., Antoniadis D. A., Fitzgerald E. A. (2005). Nanocrystalline Ge Flash Memories: Electrical Characterization and Trap Engineering. *The 5th Singapore-MIT Alliance Annual Symposium*, Singapore, (January 2005), pp. 19-20

Katsikas L., Eychmuller A., Giersig M., Weller H. (1990). Discrete excitonic transitions in quantum-sized CdS particles. *Chem. Phys. Letters,* V.172, No. 3-4, (1990) pp. 201-204

Kirchner H.O.K. (1971). Coarsening of grain-boundary precipitates. *Metall. Trans,* No. 2, (1971), pp. 2861 – 2864

Kondratyev V.V., Ustyugov Yu.M. (1987). On kinetics of decay of oversaturated solid solution under partial relaxation of inner tensions. The model of partially coherent inter-phase boundaries. *Soviet Phys. Met. Metallogr.*, V. 64, No. 5, (1987), pp. 858-866

Kreye H. (1970). Einflus von Versetzungen auf die Umlosung von Teilchen. *Zs. Metallkunde,* V. 61, No. 2, (1970), pp. 108 – 113

Kukushkin S.A., Osipov A.V. (1998). Processes of condensation of thin films (Review of actual problems). *Russian Phys. Usp.*, V. 168, No. 10 (1998), pp. 1083-1116

Ledentsov N.N., Ustinov V.M., Ivanov S.V., Meltser B.Ya., Kopyev P.S., Bimberg D., Alferov J.I. (1996). Ordered arrays of quantum dots in semiconductor matrices. *Russian Phys. Usp.*, V. 166, No. 4, (1996), pp. 423-431

Ledentsov N.N., Shchukin V.A., Grundmann M., Kirstaedter N., Böhrer J., Schmidt O., Bimberg D., Zaitsev S.V., Ustinov V.M., Zhukov A.E., Kop'ev P.S., Alferov Zh.I., Kosogov A.O., Ruvimov S.S., Werner P., Gösele U., Heydenreich J. (1996b). Direct formation of vertically coupled quantum dots in Stranski-Krastanow growth. *Phys. Rev. B*, V. 54, No. 12, (1996), pp. 8743–8750

Ledentsov N.N., Ustinov V.M., Schukin V.A., Kopyev P.S., Alferov J.I., Bimberg D. (1998). Heterostructures with quantum dots: obtaining, properties, lasers. *Russian Phys. Semicond.*, V. 32, No. 4, (1998), pp. 385-410

Leonard D., Krishnamurthy M., Reaves C.M., Denbaars S.P., Petroff P.M. (1993). Direct formation of quantum-sized dots from uniform coherent islands of InGaAs on GaAs surfaces. *Appl. Phys. Lett*, V. 63, No. 23, (1993), pp. 3203-3205

Lifshitz I.M., Slyozov V.V. (1958). On kinetics of diffusion decay of oversaturated solid solutions. *JETP*, V. 35, No. 2 (1958), pp. 479-492

Lifshitz I.M., Slesov V.V. (1961). The kinetics of precipitation from supersaturated solid solution. *J. Phys. Chem. Solids*, V. 19, No.1/2, (1961), pp. 35-50

Marquis E.A., Seidman D.N. (2001). Error! Hyperlink reference not valid.. *Acta Materialia*, V. 49, No. 10, (2001), pp. 1909-1919

Mo Y.-W., Savage D.E., Swartzentruber B.S., Lagally M.G. (1990). Kinetic pathway in Stranski-Krastanov growth of Ge on Si(001). *Phys. Rev. Lett*, V. 65, No. 8, (1990), pp. 1020-1023

Moison J.M., Houzay F., Barthe F., Leprince L., Andre E., Vatel O. (1994). Self-organized growth of regular nanometer-scale InAs dots on GaAs. *Appl. Phys. Lett,* V. 64, No. 2, (1994), pp. 196-198

Müller P., Kern R. (1998). Equilibrium shape of epitaxially strained crystals (Volmer–Weber case). *J. Cryst. Growth*, V. 193, (1998), pp. 257-270

Neizvestny I.G., Suprun S.P., Talochkin A.B., Shumsky V.N., Efanov A.V. (2001). Quantum dots of Ge in non-strained heterosystem GaAs/ZnSe/Ge/ZnSe. *Russian PTS*, V. 35, No. 9, (2001), pp. 1135-1142

Nitsche H., Sommer F., and Mittemeijer E.J. (2005). The Al nano-crystallization process in amorphous Al, Ni,Y,Co. *J. Non Cryst. Solids*, V. 351, (2005), pp. 3760-3771

Ostwald W. (1900). Über die Vermeintliche Isometric des roten undgelben Quecksilberxyds und die Oberflachenspannung fester Körper. *Z. Phys. Chem,* Bd.34, (1900), pp. 495-503

Pchelyakov O.P., Bolkhovityanov Yu.B., Dvurechensky A.V., Sokolov L.V., Nikiforov A.I., Yakimov A.I., Voightlender B. (2000). Silicon-germanium nanostructures with quantum dots: mechanisms of formation and electrical properties. *Russian Phys. Semicond.*, V. 34, No. 11, (2000), pp. 1281-1299

Reutov V.F., Dmitriev S.N. (2002). Ion-track nanotehnology. *Russian Chem. J.*, V. 46, (2002), pp. 74-80

Roko M. (2002). Prospects of development of nanotehnology: National programs, and Educational problems. *Russian Chem. J.*, V. 46, (2002), pp. 90-95

Safonov K.L., Trushin Yu.V. (2007). Criteria of transition of nanoclusters of Ge at Si from pyramidal to cupola-like form. *JTP Lett.*, V. 33, (2007), pp. 7-12

Savchuk A.I., Rudko G.Yu., Fediv V.I., Voloshchuk A.G., Gule E.G., Ivanchak S.A., Makoviy V.V. (2010a). Evolution of $CdS:Mn$ nanoparticle properties caused by pH of colloid solution and ultrasound irradiation. *Phys. Stat. Sol. (c).* V. 7, No.6, (2010), pp. 1510-1512

Savchuk A.I., Makhniy V.P., Fediv V.I., Kleto G.I., Savchuk S.A., Perrone A., Cultrera L. (2010b). Effects of co-doping in ZnO-based semimagnetic semiconductor thin films. *J. Phys.: Conference Series,* V. 8, (2010), pp. 1-4

Savchuk A.I., Fediv V.I., Ivanchak S.A., Makoviy V.V., Smolinsky M.M., Savchuk O.A., Perrone A., Cultrera L. (2010c). Formation and transformation of II-VI semiconductor nanoparticles by laser radiation. *J. Optoelectron. Adv. Mater.,* V. 12, No. 3, (2010), pp. 561-564

Shangjr Gwo, Chung-Pin Chou, Chung-Lin Wu, Yi-Jen Ye, Shu-Ju Tsai,Wen-Chin Lin, Minn-Tsong Lin. (2003) Self-Limiting Size Distribution of Supported Cobalt Nanoclusters at Room Temperature. *Phys. Rev. Letters,* V. 90, (2003), pp. 185506-185510

Shchukin V.A. and Bimberg D. (1999). Spontaneous ordering of nanostructures on crystal surfaces. *Review of Modern Physics,* V. 71, No. 4, (1999) pp. 1125-1171

Slyozov V.V. (1967). Coalescence of oversaturated solid solution under diffusion along the boundaries of blocks and dislocation lines. *Soviet Phys. Solid Staste*, V. 9, (1967), pp. 1187-1191

Slyozov V.V., Sagalovich V.V., Tanatarov L.V. (1978). Theory of diffusive decomposition of supersaturated solid solution under the condition of simultaneous operating of several mass-transfer mechanisms. *J. Phys. Chem. Solids,* V. 10, (1978), pp. 705-709

Slyozov V.B., Sagalovich V.V. (1987). Diffusion decay of solid solutions. *Soviet Phys. Usp.*, V. 151, No. 1 (1987), pp. 67-103

Stranski I.N., Krastanow L. (1937). Sitzungsberichte d. Akad. d. Wissenscaften in Wien, Abt. lib. (1937), 146. P. 797

Vengrenovich R.D. (1975). On kinetics of coalescence of disperse extractions at dislocation network. *Soviet Phys. Met. Metallogr.,* V. 39, (1975), pp. 435-439

Vengrenovich R.D. (1977). On calculation of distribution in surface disperse systems. *Ukr. J. Phys,* V. 22, No. 2, (1977), pp. 219-223

Vengrenovitch R.D. (1980a). On the bimodal distribution in disperse systems. *Phys. Stat. Sol. (a),* V. 62, (1980a) pp. 39-44

Vengrenovitch R.D. (1980b). On kinetics of coalescence in thin films. *Ukr. J. Phys.*, V. 25, No. 3, (1980b), pp. 442-447

Vengrenovich R.D. (1982). On the Ostwald ripening theory. Overview 20. *Acta Metall,* V. 20, (1982), pp. 1079 – 1086

Vengrenovich R.D. (1983). On solution of the problem of kinetics of coalescence by Ostwald. *Rep. Ukr. Acad. Sc. A*, No. 7, (1983), pp. 28 – 33

Vengrenovich R.D., Polushina I.A. (1985). Influence of the volume part of disperse phase on kinetics of coalescence under dislocation diffusion. *Soviet Phys. Met. Metallogr.,* V. 59, No. 4, (1985), pp. 650-660

Vengrenovich R.D. (1998). The size distribution function under dislocation-matrix diffusion. *Rep. Ukr. Acad. Sc. A*, No. 1, (1998), pp. 112 – 120

Vengrenovich R.D., Kovalik F.L., Foglinsky S.V. (1998). Size distribution function under dislocation-matrix diffusion. *Russian Pysics Journ.,* No. 10, (1998), pp. 25-35

Vengrenovich R.D., Gudyma Yu.V. (2001). Kinetics of optical thermal breakdown of thin semiconductor film. *Russian Phys. Solid State,* V. 43, No. 7, (2001), pp. 1171-1175

Vengrenovich R.D., Gudyma Yu.V. and Yarema S.V. (2001a). Growth of Second-Phase Particles upon the Loss of Coherency. *Russian Phys. Met. Metallogr.,* V. 91, No. 3, (2001a), pp. 228-232

Vengrenovich R.D., Gudyma Yu.V., Yarema S.V. (2001b). Ostwald's ripening of nanostructures with nanodots. *Russian Phys. Semicond.,* V. 35, No. 12, (2001), pp. 1440-1444

Vengrenovich R.D., Gudyma Yu.V. and Nikirsa d.d. (2001c). Kinetics of the photoinduced phase transition at the surface of a semiconductor with renormalized bandgar. *J. Phys.: Condens. Matter,* V. 13, (Januar 2001), pp. (2947-2953)

Vengrenovich R.D., Gudyma Yu.V. and Yarema S.V. (2002) Ostwald Ripening under dislocation diffusion. *Scripta Materialia,* V.46, No. 5, (2002), pp. 363-367

Vengrenovitch R.D., Gudyma Yu. V., Yarema S.V. (2005). Quantum dot formation in heteroepitaxial structures. *Phys. Stat. Sol. (b),* V. 242, (2005), pp. 881-889

Vengrenovich R.D., Moskalyuk A.V., Yarema S.V. (2006a). Size distribution function of islands under dislocation-surface diffusion for semiconductor structures. *Rusian Phys. Semicond.*, V. 40, No. 3, (2006), pp. 276-280

Vengrenovich R.D., Moskalyuk A.V., Yarema S.V. (2006b). Ostwald's ripening of heterostructures with quantum dots under dislocation-surface diffusion. *Ukr. J. Phys.*, V. 51, No. 3, (2006), pp. 307-310

Vengrenovich R.D., Moskalyuk A.V., Yarema S.V. (2007a). Ostwald's ripening under mixed-type diffusion, *Russian Phys. Solid State*, V. 49, No. 1, (2007), pp. (13-18)

Vengrenovich R.D., Ivanskii B.V., Moskalyuk A.V. (2007b). Generalized Lifshitz-Slyozov-Wagner distribution. *JETP*, V. 131, No. 6, (2007). pp. 1040-1047

Vengrenovich R.D., Ivans'kyi B.V., Moskalyuk A.V. (2008a). Generalized Chakraverty-Wagner Distribution. *Ukr. J. Phys.*, Vol.53, No. 11, (2008), pp. 1101-1109

Vengrenovich R.D., Ivanskii B.V., Moskalyuk A.V. (2008b). Ostwald's ripening of quantum-sized crystals under mixed diffusion. *Metalooptics and Modern Technologies*, V. 30, No. 2, (2008), pp. 247-266

Vengrenovich R.D., Ivanskii B.V., Moskalyuk A.V. (2010). Ostwald ripening of nanoislands in semiconductor heterosystemsand its influence on optical properties. *Opto-electronics Review*, V. 18, No 2, (2010), pp. 168-176.

Vostokov N.V., Gusev S.A., Dolgov I.V., Drozdov Yu.N., Krasilnik Z.F., Lobanov D.N., Moldavskaya L.D., Novikov A.V., Postnikov V.V., Filatov D.O. (2000). Elastic strains and compound of self-organized nanoislands of GeSi at Si (001). *Russian Phys. Semicond.,* V. 34, No. 1. (2000), pp .8-12

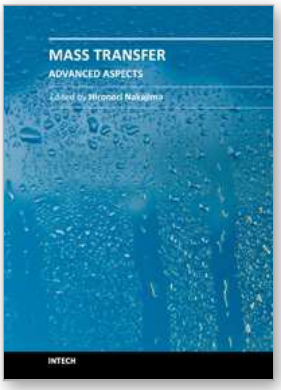
Wagner C. (1961). Theorie der Alterung von Niderschlagen durch Umlösen (Ostwald Reifung). *Zs. Electrochem.,* Bd. 65, №7/8, (1961), pp. 581 – 591

Werner P., Zakharov N.D., Gerth G., Schubert L., Gösele U. (2006). On the formation of Si nanowires by molecular beam epitaxy. *Int. J. Mat. Res. (formelly Z. Metallkd.)* V. 97, No. 7, (2006). pp. 1008-1015

Xiaofeng Lai, Todd P. St.Clair and D. Wayne Goodma. (1999). Oxygen-induced morphological changes of Ag nanoclusters supported on TiO_2(110). *Faraday Discuss.* V. 114, (1999), pp. 279-284

Xiaosheng Fang, Tianyou Zhai, Ujjal K. Gautam, Liang Li, Limin Wu, Yoshio Bando, Dmitri Golberg. (2011). ZnS nanostructures: From synthesis to applications. *Progress in Materials Science,* V. 56, (2011), pp. 175-287

Yakimov A. I., Nikiforov A. I., and Dvurechenski A. V. (2007). Bonding State of a Hole in Ge/Si Double Quantum Dots. *JETP Letters*, V. 86. (2007), pp. 478-481



Mass Transfer - Advanced Aspects

Edited by Dr. Hironori Nakajima

ISBN 978-953-307-636-2
Hard cover, 824 pages
Publisher InTech
Published online 07, July, 2011
Published in print edition July, 2011

Our knowledge of mass transfer processes has been extended and applied to various fields of science and engineering including industrial and manufacturing processes in recent years. Since mass transfer is a primordial phenomenon, it plays a key role in the scientific researches and fields of mechanical, energy, environmental, materials, bio, and chemical engineering. In this book, energetic authors provide present advances in scientific findings and technologies, and develop new theoretical models concerning mass transfer. This book brings valuable references for researchers and engineers working in the variety of mass transfer sciences and related fields. Since the constitutive topics cover the advances in broad research areas, the topics will be mutually stimulus and informative to the researchers and engineers in different areas.

How to reference

In order to correctly reference this scholarly work, feel free to copy and paste the following:

Roman Vengrenovich, Bohdan Ivanskii, Anatolii Moskalyuk, Sergey Yarema and Miroslav Stasyk (2011). Mass Transfer Between Clusters Under Ostwald's Ripening, Mass Transfer - Advanced Aspects, Dr. Hironori Nakajima (Ed.), ISBN: 978-953-307-636-2, InTech, Available from: http://www.intechopen.com/books/mass-transfer-advanced-aspects/mass-transfer-between-clusters-under-ostwald-s-ripening

INTECH
open science | open minds

InTech Europe
University Campus STeP Ri
Slavka Krautzeka 83/A
51000 Rijeka, Croatia
Phone: +385 (51) 770 447
Fax: +385 (51) 686 166
www.intechopen.com

InTech China
Unit 405, Office Block, Hotel Equatorial Shanghai
No.65, Yan An Road (West), Shanghai, 200040, China
中国上海市延安西路65号上海国际贵都大饭店办公楼405单元
Phone: +86-21-62489820
Fax: +86-21-62489821

© 2011 The Author(s). Licensee IntechOpen. This is an open access article distributed under the terms of the Creative Commons Attribution 3.0 License, which permits unrestricted use, distribution, and reproduction in any medium, provided the original work is properly cited.